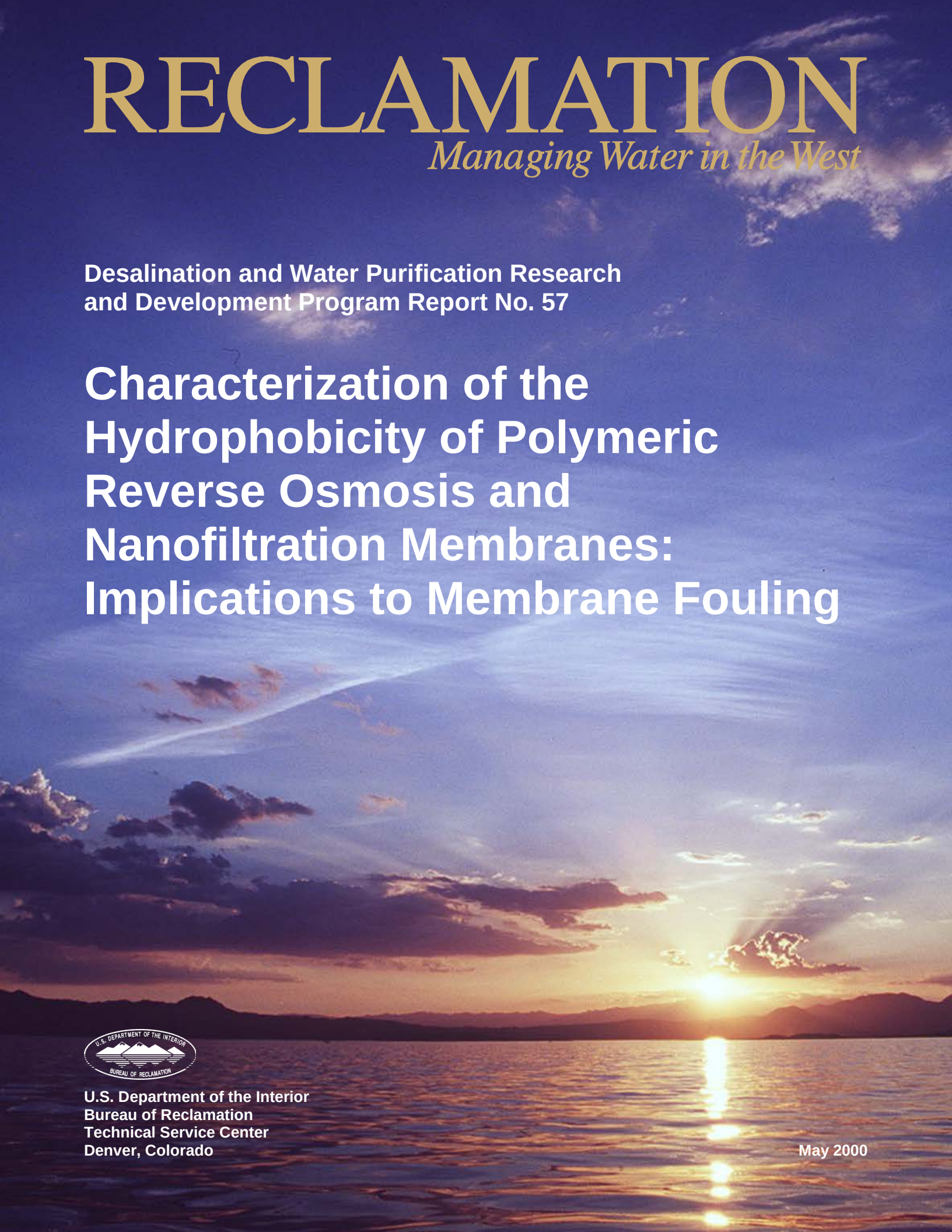

RECLAMATION

Managing Water in the West

Desalination and Water Purification Research and Development Program Report No. 57

Characterization of the Hydrophobicity of Polymeric Reverse Osmosis and Nanofiltration Membranes: Implications to Membrane Fouling

U.S. Department of the Interior
Bureau of Reclamation
Technical Service Center
Denver, Colorado

May 2000

REPORT DOCUMENTATION PAGE

Form Approved
OMB No. 0704-0188

1. REPORT DATE *(DD-MM-YYYY)*	2. REPORT TYPE	3. DATES COVERED *(From - To)*
May 2000	Final	September 2011 to January 2013

4. TITLE AND SUBTITLE
Characterization of the Hydrophobicity of Polymeric Reverse Osmosis and Nanofiltration Membranes: Implications to Membrane Fouling

5a. CONTRACT NUMBER
Agreement No 98-FC-81-0057

5b. GRANT NUMBER

5c. PROGRAM ELEMENT NUMBER

6. AUTHOR(S)
Amy Childress, Johnathan Brandt

5d. PROJECT NUMBER

5e. TASK NUMBER
Task A

5f. WORK UNIT NUMBER

7. PERFORMING ORGANIZATION NAME(S) AND ADDRESS(ES)
University of Nevada, Reno

8. PERFORMING ORGANIZATION REPORT NUMBER

9. SPONSORING/MONITORING AGENCY NAME(S) AND ADDRESS(ES)
Bureau of Reclamation
U.S. Department of the Interior
Denver Federal Center
PO Box 25007, Denver, CO 80225-0007

10. SPONSOR/MONITOR'S ACRONYM(S)
Reclamation

11. SPONSOR/MONITOR'S REPORT NUMBER(S)
DWPR Report No. 57

12. DISTRIBUTION/AVAILABILITY STATEMENT
Available from the National Technical Information Service,
Operations Division, 5285 Port Royal Road, Springfield VA 22161

13. SUPPLEMENTARY NOTES
Report can be downloaded from Reclamation Web site: http://www.usbr.gov/pmts/water/publications/reports.html

14. ABSTRACT
As fresh water supplies dwindle and awareness of contaminants rises, the need for effective water treatment technologies increases. For this reason, membrane processes for drinking water treatment are receiving increased attention. This study develops a methodology for determining membrane hydrophobicity and investigates the relationship between hydrophobicity and membrane fouling. It establishes a protocol for measuring contact angles on both cellulose acetate and thin-film composite reverse-osmosis and nanofiltration membranes. It then uses these contact angle measurements in the Lifshitz-van der Waals/Acid-Base approach to quantitatively calculate the surface energetics of the membranes.

15. SUBJECT TERMS
Reverse osmosis, nanofiltration, membrane fouling, hydrophobicity, water treatment, desalination

16. SECURITY CLASSIFICATION OF:			17. LIMITATION OF ABSTRACT	18. NUMBER OF PAGES	19a. NAME OF RESPONSIBLE PERSON
a. REPORT	b. ABSTRACT	a. THIS PAGE			Scott Irvine
U	U	U		49	19b. TELEPHONE NUMBER *(Include area code)* 303-445-2253

Desalination and Water Purification Research and Development Program Report No. 57

Characterization of the Hydrophobicity of Polymeric Reverse Osmosis and Nanofiltration Membranes: Implications to Membrane Fouling

Prepared for the Bureau of Reclamation Under Agreement No. 98-FC-81-0057

by

Amy Childress, Ph.D., and Jonathan A. Brant
University of Nevada, Reno

U.S. Department of the Interior
Bureau of Reclamation
Technical Service Center
Denver, Colorado

May 2000

MISSION STATEMENTS

The U.S. Department of the Interior protects America's natural resources and heritage, honors our cultures and tribal communities, and supplies the energy to power our future.

The mission of the Bureau of Reclamation is to manage, develop, and protect water and related resources in an environmentally and economically sound manner in the interest of the American public.

Disclaimer

The views, analysis, recommendations, and conclusions in this report are those of the authors and do not represent official or unofficial policies or opinions of the United States Government, and the United States takes no position with regard to any findings, conclusions, or recommendations made. As such, mention of trade names or commercial products does not constitute their endorsement by the United States Government.

Acknowledgments

This research was funded by the U.S. Department of the Interior, Bureau of Reclamation, Desalination and Water Purification Research and Development Program. The assistance of Kim Linton throughout the study is greatly appreciated.

CONTENTS

Page

Figures

Page

Tables

Page

ACRONYMS AND ABBREVIATIONS

AB	polar acid-base interactions
LW	apolar Lifshitz-van der Waals surface energy component
M	moles
mJ/m^2	millijoules per square meter
mM	millimoles
NF	nanofiltration
PHA	peat humic acid
psi	pounds per square inch
RO	reverse osmosis
UF	ultrafiltration
γ	total interfacial tension between phases
ΔG	free energy of interaction between two phases
µg/L	micrograms per liter
µL	microliter

METRIC CONVERSIONS

The metric equivalents for non-metric units used in the text are as follows:

Unit	Metric equivalent
1 gallon	3.785 liters
1 gallon per minute	3.785 liters per minute
1 gallon per square foot of membrane area per day	40.74 liters per square meter per day
1 inch	2.54 centimeters
1 pound per square inch	6.895 kilopascals

1 INTRODUCTION

As fresh water supplies dwindle and awareness rises concerning the effects of inorganic (e.g., arsenic), organic (e.g., disinfection byproduct precursors), and microbiological (e.g., giardia and cryptosporidium) contaminants, the need for more effective drinking water treatment technologies increases (Glater 1998). For this reason, further development of membrane processes for drinking water treatment is being pursued (Glater 1998). Membrane processes have several advantages over conventional water treatment processes (Williams et al. 1992, Belfort et al. 1994). Most notable is the superior quality of the product water that is produced without using expensive chemical additives, which may produce adverse health effects. As membrane processes continue to grow as a water treatment alternative, research that investigates methods to optimize membrane performance must be pursued.

The phenomenon of membrane fouling hinders membrane performance and shortens membrane life (Hong and Elimelech 1997). Membrane fouling results from the attachment, accumulation, or adsorption of substances onto the membrane surface and/or within the membrane pores (Zhu and Elimelech 1995). Fouling mechanisms vary based on the physical structure and surface chemistry of a membrane. For example, pore plugging is a major mechanism in the fouling of looser ultrafiltration (UF) but its role in the fouling of tighter reverse osmosis (RO) membranes is relatively insignificant (Zhu and Elimelech 1995). However, for both porous and nonporous membranes, physical and chemical interactions between solutes or particles and the membrane surface substantially affect the rate at which membrane fouling occurs (Reihanian et al. 1983, Oldani and Schock 1989, Capannelli et al. 1990, Nyström et al. 1990, Gekas et al. 1992, Gourley et al. 1994, Zhu and Elimelech 1995, Bouchard et al. 1997, Elimelech et al. 1997, Nabe et al. 1997, Zhu and Elimelech 1997). Therefore, development of RO and nanofiltration (NF) membranes with improved performance capabilities (i.e., lower fouling rates) requires a comprehensive understanding of the complex interactions occurring at the membrane surface. Determination of the surface energy properties of a membrane is a first step in achieving this understanding.

Contact angle measurements are a common and relatively easy method to characterize the surface properties of water treatment membranes (Grundke et al. 1996, Kwok and Neumann 1999). Van Oss (1993) developed a method for calculating the surface energy components of a solid surface from contact angles. Three probe liquids are used to develop three equations that are solved simultaneously. This method is most often referred to as the Lifshitz-van der Waals/Acid-Base approach. Using this approach, it is possible to calculate the solid surface energy components and the free energy of hydrophobic interaction between a surface and a liquid (van Oss 1993). In previous investigations, the hydrophobicity of membrane surfaces has only been approximated by contact angle measurement.

The hydrophobic nature of a membrane estimated from its contact angle with water has previously been correlated with membrane fouling (Capannelli et al. 1990, Zhang and Hallström 1990, Gekas et al. 1992, Gourley et al. 1994, Bouchard et al. 1997, Nabe et al. 1997). In all previous investigations it has been shown that hydrophobic membranes tend to foul more rapidly than hydrophilic membranes (Capannelli et al. 1990, Nyström et al. 1990, Gekas et al. 1992, Gourley et al. 1994, Kulkarni et al. 1996, Mukherjee et al. 1996, Nabe et al. 1997). Additionally, it has been shown that membrane fouling can be reduced through the hydrophilization of UF (Capannelli et al. 1990, Gekas et al. 1992, Nabe et al. 1997) and RO (Kulkarni et al. 1996, Mukherjee et al. 1996) membrane surfaces. Therefore, quantification of membrane hydrophobicity provides valuable insight into the fouling behavior of water treatment membranes.

The primary goal of this investigation was to characterize the hydrophobicity of five water treatment membranes and to perform preliminary membrane performance tests to evaluate possible relationships between membrane hydrophobicity and membrane fouling. The sub-objectives of this goal were:

1. To establish protocol for measuring the contact angle of polymeric RO and NF membranes.
2. To perform contact angle measurements on several cellulose acetate and thin-film composite water treatment membranes.
3. To use the contact angle results for the quantitative determination of membrane hydrophobicity.
4. To perform preliminary membrane performance tests and evaluate possible relationships between membrane hydrophobicity and membrane fouling.

In achieving these objectives, four questions will be addressed.

1. Does the general trend for contact angle measurements with water (which are simpler to perform than hydrophobicity measurements) agree with the general trend for membrane hydrophobicity? Are contact angle measurements with water an adequate surrogate for hydrophobicity measurements?
2. What role does membrane hydrophobicity play in permeate flux decline?
3. Can actual correlations be drawn between membrane hydrophobicity and membrane performance, i.e., do significant trendlines exist?
4. How can membrane hydrophobicity data best be used in predicting flux decline behavior?

2 BACKGROUND AND RELATED RESEARCH

2.1 Definition of Contact Angle

Contact angle is a measure of the wettability of a solid surface (Young 1805, Hamilton 1972, Good 1979, Oldani and Schock 1989, Grundke et al. 1996, Decker et al., 1999). Contact angle can also be used to determine the surface tension components and hydrophobic nature of a solid surface (Good 1979). When a drop of liquid is placed on a dry membrane surface, the contact angle is the angle that develops between the membrane surface and the air/liquid interface. The contact angle is formed at the junction of the three phases (i.e., the solid, liquid and gas phases) and is measured through the denser fluid phase. Figure 1 illustrates the contact angle of a liquid drop on a solid surface; the contact angle is measured through the liquid phase.

2.2 Methods of Measuring Contact Angles

Several methods have been developed to measure contact angles. Three of the more common methods are the sessile drop method (Cuperus and Smolders 1991), the immersion method (Rosa and de Pinho 1997), and the captive bubble method (Zhang and Hallström 1990). The advantages and disadvantages of each method are discussed below.

2.2.1 Sessile Drop

The sessile drop technique is the simplest of the three methods in terms of measurement procedure. The sessile drop technique consists of placing a liquid drop on a dry surface exposed to the surrounding air and measuring the contact angle that the drop makes with the membrane surface (Figure 1).

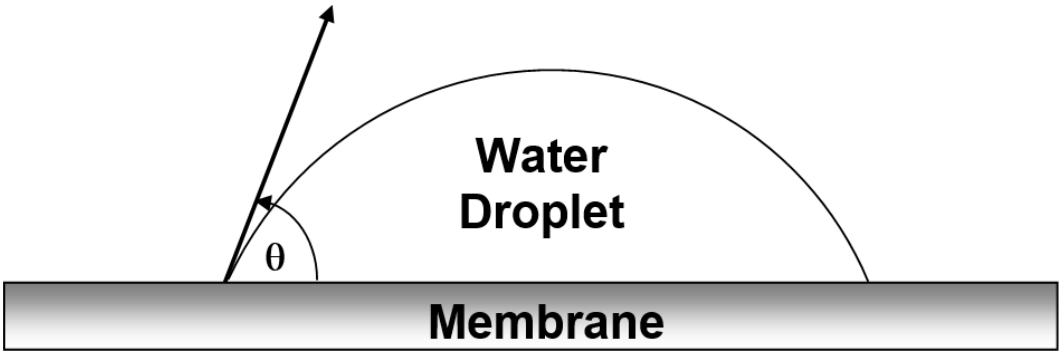

Figure 1.—Contact angle of a liquid drop on a solid surface (the sessile drop technique).

Although this method is the easiest of the three to perform it has a number of critical drawbacks when applied to the study of water treatment membranes. Because the liquid drop is exposed to the surrounding air it is affected by evaporation (Dahlgren et al. 1986). A liquid drop on a surface will evaporate at a rate proportional to the air's humidity (Dahlgren et al. 1986). Because a small volume of liquid (~10 µL) is typically used during testing, the rate of evaporation can be substantial. A 50% decrease in volume (from 10 µL to 5 µL) in a 10-min period for a hydrophilic surface and in a 30-min period for a hydrophobic surface has been observed (Dahlgren et al. 1986). As the volume of the liquid drop decreases, its contact angle changes and becomes difficult to determine.

Additional concerns of the sessile drop method stem from the fact that the membrane must be dry. First, it has been demonstrated that drying of membranes irreversibly damages the morphological structure of the membrane, especially in the case of cellulose acetate membranes prepared by phase inversion (Rosa and de Pinho 1997). Second, when a liquid drop is placed on a dry membrane surface, the portion of the membrane exposed to the liquid swells and changes structure (Kwok et al. 1997). Changes in the membrane's structure due to drying or hydration affect the values of the solid-liquid and solid-vapor surface tensions and thereby alter the measured contact angle (Kwok et al. 1997). Third, membrane surface porosity and roughness also have a greater effect on contact angle measurements performed using the sessile drop method (Rosa, M.J., and M.N. de Pinho.1997. In the dry state, contact angle measurements on porous membranes are greatly affected by capillary penetration of the liquid drop. This produces contact angles that are not representative of the bulk solid.

2.2.2 Immersion Method

The immersion method has only recently been developed for performing contact angle measurements on membrane surfaces. The general procedure consists of placing a drop of a neutral organic on a membrane coupon immersed in water (Keurentjes et al. 1989). The organic must be immiscible in water and heavier than water. The organic is injected into the water and allowed to come to rest on the solid surface before the contact angle is measured. Following the equilibration period, the contact angle between the organic and the solid surface is measured. There are several advantages to using the immersion method when performing contact angle measurements on water treatment membranes. The principal advantage is that the risky and time consuming drying process associated with the sessile drop method is avoided (Rosa and de Pinho 1997). The main drawback of the immersion method is in the selection of an organic that is immiscible in water and heavier than water. Rosa and de Pinho (1997) recommend using carbon tetrachloride. However, usage of carbon tetrachloride requires special laboratory procedures and poses serious health risks.

2.2.3 Captive Bubble Method

The captive bubble method has proven to be a viable method for obtaining reproducible data in characterizing membrane surface properties (Zhang and Hallström 1990). The captive bubble method is similar to the immersion method in that the membranes are analyzed in an aqueous environment. The captive bubble method measures the contact angle an air bubble makes on an inverted membrane surface immersed in a probe liquid (Figure 2).

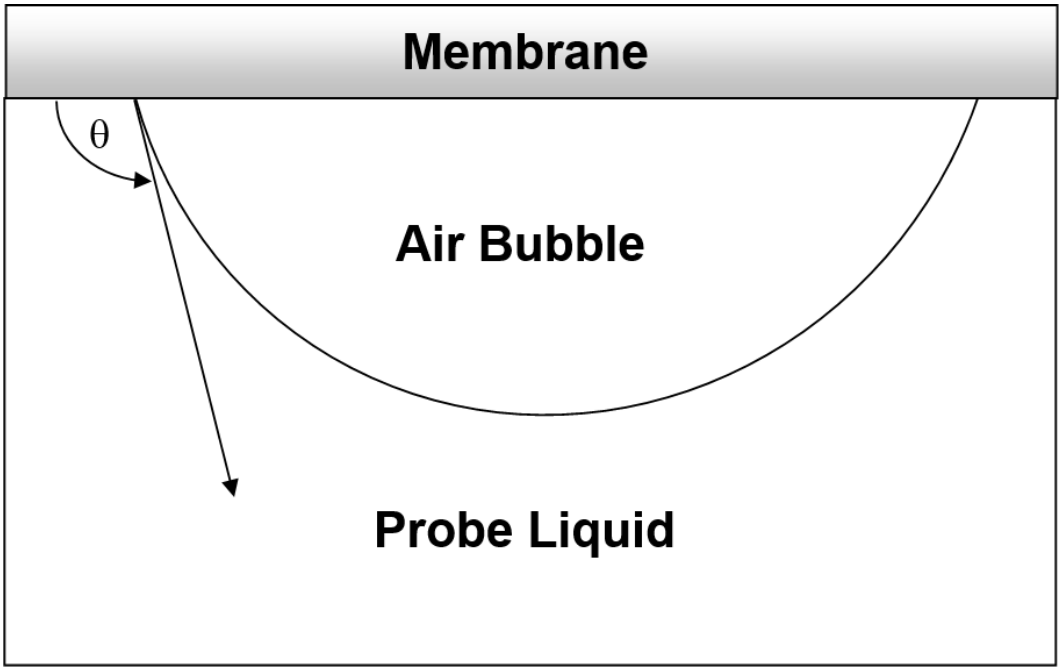

Figure 2.—Contact angle of an air bubble on a solid surface (the captive bubble technique).

Because the membrane sample is immersed in solution and is completely hydrated, the contact angle measurement is less influenced by pores and swelling (Kwok et al. 1996, Rosa and de Pinho 1997); also its actual operating conditions are better simulated (Zhang and Hallström 1990). There are no health and safety concerns as with the carbon tetrachloride in the immersion method. And finally, contact angle hysteresis is limited using the captive bubble method as hysteresis is less prominent in liquid-solid-gas systems compared to liquid-liquid-solid systems (Good 1979). For these reasons, the captive bubble method was selected for the current investigation.

In the captive bubble method, the membrane coupons are mounted on the underneath side of a stainless steel plate with the active layer facing down. The plate is lowered into a quartz cell that houses the probe liquid. An air bubble is delivered to the membrane surface using a syringe with a bent needle attachment. There are two methods for delivering the air bubble to the membrane surface: the

dynamic method and the static method (Drelich and Miller 1994). The two methods differ by the nature of bubble delivery and attachment to the membrane surface (Drelich and Miller 1994). In the dynamic method, air bubbles are released below the membrane surface and become captured on the membrane surface by the bubble's own buoyant force (Drelich and Miller 1994). In the static method, the air bubble is placed directly on the membrane surface and doesn't float through the probe liquid (Drelich and Miller 1994). For the static method, the needle remains in the air bubble for the duration of the contact angle measurement (Drelich and Miller 1994). When the needle is penetrating the air bubble, the bubble's shape may be distorted. Also, the surface tension of the liquid solution may cause the air bubble to attach to the needle and rise up the length of the needle. The overall effect may be a distorted bubble shape and an inaccurate contact angle measurement. Therefore, the dynamic method has been selected for the current investigation.

2.3 Types of Contact Angles

Three different types of contact angles can be measured. These include the advancing, receding, and equilibrium contact angles. In the current investigation, the equilibrium contact angle was measured. The equilibrium contact angle is defined as the contact angle that does not change with time. The volume of the air bubble remains constant and thus the contact angle is constant (Drelich et al. 1996). Once the equilibrium contact angle is reached, the three phases (i.e., the solid, liquid, and gas phases) are said to be in thermodynamic equilibrium (Marmur 1996). The equilibrium contact angle corresponds to the absolute minimum in surface energy available, or the stable state (Marmur 1996). In contrast, both the advancing and receding contact angles are metastable; external energy sources, such as vibrations, can cause the contact angle to move from one metastable state to the next (Marmur 1996).

2.4 Theory of Contact Angle and Hydrophobicity

2.4.1 Free Energy of Interaction

Contact angles can be used to determine the surface energy components of a solid surface (Good 1979, Gourley et al. 1994). When a liquid comes in contact with a solid surface, three interfaces are formed: the solid-liquid, solid-gas, and liquid-gas interfaces. The surface energies, or surface tensions, of the solid and liquid phases characterize the contact angle that is formed (Drelich and Miller 1994, Bouchard et al. 1997). Surface energy and surface tension are used interchangeably to describe a force that exists on a surface and acts perpendicular and inward from the boundaries of the surface, thus decreasing the area of the surface (Hiemenz 1986). The surface energies of solid and liquid phases determine the interfacial energy, or the free energy of interaction (ΔG) between the two phases. It is the interfacial free energy, or free energy of hydrophobic

interaction of a surface that determines its hydrophobic nature. The free energy of interaction between the two phases produces the contact angle that is formed.

The free energy of interaction between two molecules or particles (phase 1) immersed in a liquid (phase 2) may be expressed following the Dupre equation (van Oss 1993):

$$\Delta G_{121} = -2\gamma_{12} \quad (1)$$

where ΔG_{121} is the free energy of interaction between phases 1 and 2
γ_{12} is the total interfacial tension between phases 1 and 2

Using equation 1 several observations can be made concerning the interaction between two particles or phases. When $\gamma_{12} < 0$ or $\Delta G_{121} > 0$, the two phases tend to repulse one another, thus demonstrating that phase 1 would remain stable if immersed in phase 2 (van Oss 1993). Plainly, the opposite condition (i.e., $\gamma_{12} > 0$ or $\Delta G_{121} < 0$) signifies an attraction between the two phases, hence phase 1 would be unstable if immersed in phase 2 (van Oss 1993).

2.4.2 Young's Equation

Contact angle theory is based on an equation developed by Young (1805). Young's equation represents the equilibrium relationship of a liquid drop on a solid surface as a function of three interfacial tensions: solid-vapor (γ_{sv}), solid-liquid (γ_{sl}), and liquid-vapor (γ_{lv}) (Figure 3) (Bouchard et al. 1997, Kwok and Neumann 1999).

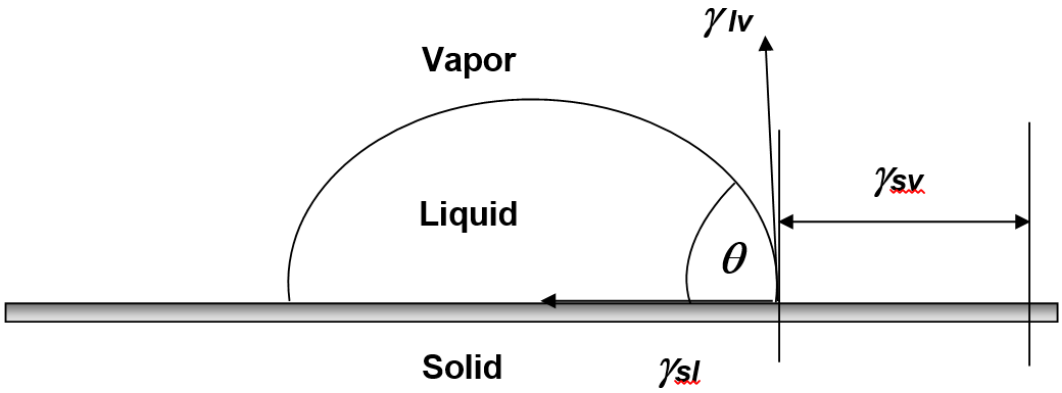

Figure 3.—Schematic of the relationship between the contact angle and surface energy components of a three phase (solid, liquid, and vapor) system.

Young's equation was developed for ideal systems in thermodynamic equilibrium (Good 1979, Oldani and Schock 1989, Zhang and Hallström 1990). Although numerous forms of Young's equation have been developed, the following form is most commonly used when performing contact angle analysis (Oldani and Schock 1989):

$$\gamma_s^{TOT} = \gamma_{sl}^{TOT} + \gamma_l^{TOT} \cos\theta \quad (2)$$

where
γ_s^{TOT} is the total free energy of the solid phase
γ_l^{TOT} is the total free energy of the liquid phase
γ_{sl}^{TOT} is the total free energy of the solid-liquid interface
θ is the equilibrium contact angle

Young's equation illustrates the relationship between the adhesion of the liquid to the solid surface and the cohesion of the liquid to itself (Extrand 1998, Wolansky and Marmur1998). In Young's equation the term $\gamma_l \cos\theta$ is often referred to as the wetting tension, or the adhesion tension (Good 1979). In other words, this term gives the surface tension value for the liquid solution at which it will wet, or adhere to the solid surface. When the self cohesion of the liquid is greater than the adhesion of the liquid to the solid, a large contact angle is formed (Extrand 1998). As the self-cohesion of the liquid decreases the contact angle that the liquid forms on the solid decreases (Extrand 1998). When the adhesion of the liquid to the solid is much greater than the self-cohesion of the liquid, a small contact angle is formed (Extrand 1998).

2.4.3 Fowkes' Approach

The surface energy properties of a solid cannot be measured directly as with liquids. Instead, solid surface energetics can be determined using the known surface energy values of a liquid and an energy balance between the solid and liquid (van Oss 1993). The first to use this method was Fowkes (1964). Fowkes (1964) stated that the total surface energy of a respective phase (solid or liquid) can be expressed as a summation of its two surface energy components:

$$\gamma^{TOT} = \gamma^{d} + \gamma^{n} \quad (3)$$

where
γ^{TOT} is the total surface free energy
γ^{d} is the dispersive surface energy component
γ^{n} is the non-dispersive surface energy component

The dispersive energy component specifically results from molecular interaction due to London forces. The non-dispersive energy component is an inclusive term describing all interactions due to non-London forces. Non-London forces include hydrogen and dipole-dipole interactions.

Using equation 3, the interaction between two phases, a solid and a liquid, can be expressed using a geometric mean relationship for the dispersive energy components of the solid and liquid phases:

$$\gamma_{sl}^{TOT} = \gamma_s^{TOT} + \gamma_l^{TOT} - 2\sqrt{\gamma_s^d \gamma_l^d} \quad (4)$$

where γ_s^d is the dispersive surface energy component of the solid
γ_l^d is the dispersive surface energy component of the liquid

Inserting equation 4 into Young's equation (equation 2) produces:

$$\gamma_l^{TOT} \cos\theta = -\gamma_l^{TOT} + 2\sqrt{\gamma_s^d \gamma_l^d} \quad (5)$$

Applying equation 5 to actual systems provides a means to calculate the surface energy properties of a solid surface using the known surface properties of a liquid and the contact angle of the liquid with the solid. However, as evident from equation 5, Fowkes' (1964) method only applies to solid surfaces that are strictly dispersive ($\gamma_s = \gamma_s^d$). Therefore, this method is rather limited in its ability to characterize typical solid surfaces.

2.4.4 Lifshitz–van der Waals/Acid-Base Approach

A generalization of the Fowkes approach to surface characterization was developed by van Oss et al. (1986b). van Oss et al. (1986b) clarified the general surface energy components proposed by Fowkes (1964). The dispersive forces cited by Fowkes were ascribed solely to the apolar Lifshitz-van der Waals (LW) surface energy component. The non-dispersive forces cited by Fowkes were ascribed to polar acid-base (AB) interactions at a surface due to hydrogen bonding. The result was the following expression for the total energy of a surface:

$$\gamma^{TOT} = \gamma^{LW} + \gamma^{AB} \quad (6)$$

where γ^{LW} is the Lifshitz-van der Waals component of surface energy
γ^{AB} is the acid-base component of surface energy

This modification is referred to as the Lifshitz-van der Waals/Acid-Base approach. The Lifshitz-van der Waals/Acid-Base approach has been widely used as a method for determining surface tension components of a solid and interfacial free energies between two phases (Kwok and Neumann 1999).

The non-polar LW force represents a single electrodynamic property of a given material. Conversely, the polar AB force is comprised of two non-additive electron-acceptor and electron-donor components (van Oss 1993). The polar AB component of a material's surface energy is thus given by (van Oss and Good 1988, Bouchard et al. 1997):

$$\gamma^{AB} = 2\sqrt{\gamma^+ \gamma^-} \quad (7)$$

where γ^+ is the electron-acceptor component
γ^- is the electron-donor component

Substituting equation 7 into equation 6 produces the following expression for the total surface energy of a respective phase:

$$\gamma^{TOT} = \gamma^{LW} + 2\sqrt{\gamma^{+}\gamma^{-}} \tag{8}$$

Division of the AB force into two components demonstrates the fact that a polar liquid molecule may be adsorbed onto a polar surface either by its positive or negative pole (Bouchard et al. 1997). The polar interaction between two particles (particle 1 and particle 2) is described based on these two components. The electron-acceptor of particle 1 interacts with the electron-donor of particle 2 and the electron-donor of particle 1 interacts with the electron-acceptor of particle 2 (van Oss 1993). Therefore, the polar interfacial free energy existing between particles 1 and 2 can be expressed by (vanOss and Good 1988):

$$\Delta G_{12}^{AB} = -2\left(\sqrt{\gamma_1^{+}\gamma_2^{-}} + \sqrt{\gamma_1^{-}\gamma_2^{+}}\right) \tag{9}$$

where ΔG_{12}^{AB} is the free energy of interaction between polar materials 1 and 2
γ_1^{+} is the electron-acceptor component of particle 1
γ_2^{+} is the electron-acceptor component of particle 2
γ_1^{-} is the electron-donor component of particle 1
γ_2^{-} is the electron-donor component of particle 2

Based on the Dupre equation (equation 1) the interaction between two polar materials can be expressed as:

$$\gamma_{12}^{AB} = \Delta G_{12}^{AB} + \gamma_1^{AB} + \gamma_2^{AB} \tag{10}$$

where γ_{12}^{AB} is the acid-base interaction energy between particles 1 and 2
γ_1^{AB} is the acid-base energy component of particle 1
γ_2^{AB} is the acid-base energy component of particle 2

Substituting equations 7 and 9 into equation 10 yields the following formulation for the polar interfacial free energy between particles 1 and 2:

$$\gamma_{12}^{AB} = 2\left(\sqrt{\gamma_1^{+}\gamma_1^{-}} + \sqrt{\gamma_2^{+}\gamma_2^{-}} - \sqrt{\gamma_1^{+}\gamma_2^{-}} - \sqrt{\gamma_1^{-}\gamma_2^{+}}\right) \tag{11}$$

The apolar interfacial free energy between particles 1 and 2 may be expressed using (van Oss 1993):

$$\gamma_{12}^{LW} = \left(\sqrt{\gamma_1^{LW}} - \sqrt{\gamma_2^{LW}}\right)^2 \tag{12}$$

Where γ_{12}^{LW} is the Lifshitz-van der/Waals Acid-Base interfacial free energy between particles 1 and 2
γ_1^{LW} is the apolar energy component of particle 1
γ_2^{LW} is the apolar energy component of particle 2

Substituting equations 11 and 12 into equation 6 produces the following expression for the total interfacial free energy between particles 1 and 2:

$$\gamma_{12} = \left(\sqrt{\gamma_1^{LW}} - \sqrt{\gamma_2^{LW}}\right)^2 + 2\left(\sqrt{\gamma_1^+\gamma_1^-} + \sqrt{\gamma_2^+\gamma_2^-} - \sqrt{\gamma_1^+\gamma_2^-} - \sqrt{\gamma_1^-\gamma_2^+}\right) \tag{13}$$

where γ_{12} is the total interfacial tension between particles 1 and 2

Combining equations 1, 6, 7, 8, and 12 results in an equation for the interfacial free energy between a solid and a liquid:

$$\Delta G_{sl} = 2\left(\sqrt{\gamma_s^{LW}\gamma_l^{LW}} + \sqrt{\gamma_s^+\gamma_l^-} + \sqrt{\gamma_s^-\gamma_l^+}\right) \tag{14}$$

where, ΔG_{sl} is the interfacial free energy between a solid and a liquid
γ_s^{LW} is the Lifshitz-van der Waals component of the solid phase
γ_1^{LW} is the Lifshitz-van der Waals component of the liquid phase
γ_s^+ is the electron-acceptor component of the solid phase
γ_s^- is the electron-donor component of the solid phase
γ_l^+ is the electron-acceptor component of the liquid phase
γ_l^- is the electron-donor component of the liquid phase

The interaction between a solid and a liquid can also be described in terms of the contact angle between them. This equation is known as the Young-Dupre equation (van Oss 1993):

$$(1 + \cos\theta)\gamma_l^{TOT} = -\Delta G_{sl} \tag{15}$$

where γ_l^{TOT} is the total free energy of the liquid

Combining equations 14 and 15 results in the Extended Young equation, which relates the contact angle of a liquid on a solid surface to the surface energy parameters of both the solid and the liquid (van Oss and Good 1988, Gourley et al. 1994, Bouchard et al. 1997):

$$(1 + \cos\theta)\gamma_l^{TOT} = 2\left(\sqrt{\gamma_s^{LW}\gamma_l^{LW}} + \sqrt{\gamma_s^+\gamma_l^-} + \sqrt{\gamma_s^-\gamma_l^+}\right) \tag{16}$$

The Extended Young (equation 16) is best described as an equilibrium force balance. The left hand side, or the free energy of cohesion of the liquid (L), is equal to the right hand side, or the free energy of adhesion between the liquid (L) and the solid (S) (van Oss 1993, Wolansky and Marmur 1998).

Based on the Extended Young equation, the surface energy parameters of a solid surface (γ_s^{LW}, γ_s^+, γ_s^-) can be determined by performing contact angle measurements using three probe liquids with known surface energy parameters (γ_l^{LW}, γ_l^+, γ_l^-) (van Oss, 1993). Two of the probe liquids should be polar and one of the probe liquids should be apolar. The apolar liquid is used to calculate the non-polar, γ_s^{LW}, component of a solid (Ko et al. 1981, van Oss, 1993). Furthermore, high energy (apolar and polar) liquids are recommended to improve contact angle accuracy due to the large contact angles that are formed (Ko et al. 1981).

After the surface energy components (γ_s^{LW}, γ_s^+, γ_s^-) are determined from equation 16, they can then be substituted into equation 17 to calculate the interfacial free energy (ΔG) between a solid and liquid (van Oss 1993):

$$\Delta G_{sl} = -2\left(\sqrt{\gamma_s^{LW}} - \sqrt{\gamma_l^{LW}}\right)^2 - 4\sqrt{\gamma_s^+\gamma_s^-} + \sqrt{\gamma_l^+\gamma_l^-} - \sqrt{\gamma_s^+\gamma_l^-} - \sqrt{\gamma_s^-\gamma_l^+} \quad (17)$$

2.4.5 Deviations from Young's Equation

Young's equation was developed for an ideal solid surface (Good 1979, Zhang and Hallström 1990). An ideal solid surface must be smooth at the molecular level, chemically homogeneous, rigid, non-reactive, and insoluble (Good 1979, Zhang and Hallström 1990, Marmur 1996). The contact angle of a pure probe liquid on an ideal surface is called the intrinsic contact angle, or the true contact angle, for the given solid (Marmur 1996). It is only when an ideal solid surface and a pure liquid are used, that Young's equation is truly descriptive of the solid's surface energetics.

With the exception of cleaved mica, ideal surfaces are very rare (Good 1979). Most surfaces have some degree of heterogeneity and roughness (Good 1979). Chemical heterogeneity of a solid surface creates strips of wettable (hydrophilic) and non-wettable (hydrophobic) areas (Drelich and Miller 1994). A liquid droplet will align itself on those areas that are the most hydrophilic or wettable, thus creating the condition where the observed contact angle is not representative of the true surface (Extrand and Kumagai 1996). This facilitates a condition where the surface energy is not the sole determiner of the observed contact angle.

The presence of pores and the physical roughness of a membrane surface also cause the measured contact angle to deviate from the intrinsic contact angle (Good 1979, Keurentjes et al. 1989, Drelich et al. 1996). The contact angle that is most often measured is the apparent contact angle, which does not account for surface roughness. Membrane surface roughness may be on the order of several micrometers (Keurentjes et al. 1989) and can be increased through improper handling. As the liquid advances on an inclined surface (e.g., the ridge of a rough surface), a larger apparent contact angle is formed (Extrand and Kumagai 1996, Good 1979). The apparent contact angle becomes larger as the edge of the liquid drop becomes more horizontal as it travels up the incline of the surface indentation or elevation.

Deviations from an ideal surface may also result from contamination during the construction and handling of the membrane. Surface contaminants often bear little resemblance to the bulk solid and can therefore lead to increased chemical heterogeneity. Surface contamination may also lead to increased surface roughness.

2.4.6 Defining Hydrophobic Interactions

The term hydrophobic interaction, or the hydrophobic effect, is defined as the tendency of apolar chains, solutes or particles to aggregate when they are immersed in water. Often, hydrophobic surfaces are thought of as water repelling, as water forms a large (>90°) contact angle on a hydrophobic surface (Good 1979). However, using the word hydrophobic to mean water repelling is a misnomer as even aliphatic hydrocarbons ($\Delta G_{sw} \approx -40$ to -50 mJ/m^2) strongly attract water (van Oss 1993). The negative free energy signifies the strong hydrophobic nature of the aliphatic hydrocarbons.

The major and usually sole driving force for hydrophobic interactions between apolar particles when immersed in water is the strong polar (AB) energy of cohesion between water molecules. In most cases, close to 99%, and almost always more than 90% of the free energy of hydrophobic attractions between apolar molecules immersed in water (ΔG_{iwi}) is due to the hydrogen bonding component of the energy of cohesion of water: $\Delta G_{sw}^{AB} = -102$ mJ/m^2 at 200 °C (van Oss 1993). Therefore, hydrophobic interactions are a consequence of the hydrogen bonding component of the surrounding water rather than van der Waals attraction between “hydrophobic” chains, solutes, or particles. It should be made clear that hydrophobic interactions are bonds that are not of a fundamentally different physicochemical nature from van der Waals or hydrogen bonds (van Oss et al. 1986a). Hydrophobic interactions play a crucial role in the stability of particle suspensions, the stability of biopolymers, and the formation of micelles.

2.5 Hydrophobicity and Membrane Performance

Membrane surface chemistry plays a key role in determining membrane performance (Oldani and Schock 1989, Zhang and Hallström 1990, Gourley et al. 1994, Bouchard et al. 1997, Nabe et al. 1997, Rosa and de Pinho 1997). Specifically, membrane hydrophobicity can provide insight into critical aspects of membrane performance (Oldani and Schock 1989, Capannelli et al. 1990, Gourley et al. 1994, Nabe et al. 1997, Sata et al. 1998). First, hydrophobicity describes surface characteristics that govern the interaction of a liquid with a solid surface. Second, membrane hydrophobicity directly affects the interaction of organic and inorganic colloidal substances with a membrane surface (Oldani and Schock 1989, Capannelli et al. 1990, Gourley et al, 1994, Nabe et al. 1997). Third, hydrophobicity affects ion transport through the membrane (Sata et al. 1998).

A membrane can be classified as either having a high surface free energy (hydrophilic) or as having a low surface free energy (hydrophobic) (Good 1979). Membranes can be loosely characterized into one of three categories of hydrophobicity (Figure 4).

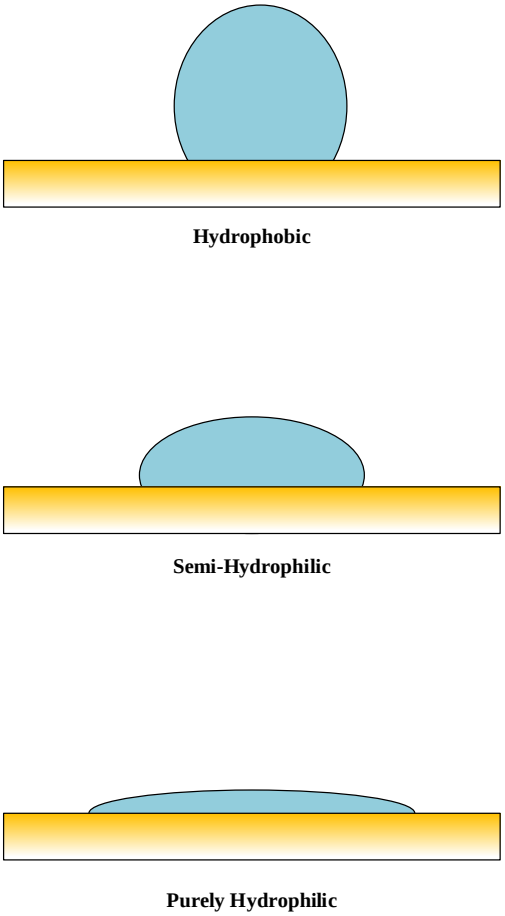

Figure 4.—Three categories of hydrophobicity

It should be noted that the contact angle ranges described below are only useful as general guidelines; exact contact angle ranges for hydrophobic and hydrophilic surfaces do not exist.

1. ***Purely Hydrophilic Surfaces*** (Figure 4a): When the contact angle of a liquid on a solid surface equals 0° the solid is said to be wet-out by the liquid. In other words the liquid will spread over the surface of the solid to form a monomolecular film (Bear 1979). Solids exhibiting such a condition are purely hydrophilic. An example of a purely hydrophilic surface is glass. If the glass is completely free of any surface contamination and is perfectly smooth, a drop of pure water would spread across the glass surface.
2. ***Semi-Hydrophilic Surfaces*** (Figure 4b): When the contact angle of a liquid on a solid surface is greater than 0° but less than 90° the liquid is said to wet the solid, but not completely (Bear 1979). In essence the solid prefers to be covered by the liquid as opposed to the surrounding gas. Therefore, solids falling within this range are primarily hydrophilic. Most commercial water treatment membranes are generally classified as semi-hydrophilic.
3. ***Hydrophobic Surfaces*** (Figure 4c): When the contact angle of a liquid on a solid surface falls within the range of 90° to 180° the liquid is said to not-wet the solid surface (Adamson 1960). It must be noted, however, that it would be nearly impossible for a liquid to achieve a contact angle of 180° because surfaces are rarely uniform in chemical and physical structure (Good 1979). By not wetting the surface, the liquid remains as a semi-spherical bubble resting on the solid surface (Bear 1979). A high surface tension liquid (e.g., water) on a low surface energy solid (e.g., teflon) favors this condition (Bear 1979, Oldani and Schock 1989). Non-wetting solids are referred to as hydrophobic.

Hydrophobic membranes are more prone to fouling than hydrophilic membranes because hydrophobic membranes prefer to be covered with colloids than with water (Hiemenz, 1986, Gourley et al. 1994). For this reason, determination of membrane hydrophobicity is critical to membrane fouling research. By characterizing membrane hydrophobicity it becomes possible to maximize contaminant removal while extending the membrane life via a reduction in fouling rate and cleaning frequency (Bouchard et al. 1997).

2.6 Previous Studies on the Determination of Membrane Surface Energetics

Few studies (e.g., Ko et al. 1981, Keurentjes et al. 1989, Gourley et al. 1994) have been performed to determine membrane surface energetics. Ko et al. (1981) used contact angles to characterize several polymeric surfaces with varying degrees of hydrophobicity. Contact angles were measured using two methods: the sessile drop method with three different drop sizes to simulate an advancing contact

angle and the submerged bubble method using n-octane bubbles. This investigation was among the first to use the Young-Dupre equation to solve for the surface energy components of a solid surface. Keurentjes et al. (1989) used a sticking bubble technique to determine the surface tension of a probe liquid at which an air bubble has a 50% chance of sticking to a membrane surface. The membranes studied were polypropylene, polytetrafluoroethylene, polydimethyl-siloxane, polysulfone, and polyethersulfone membranes. It was concluded that the critical surface tension, as it was termed, represented a measurable value for membrane hydrophobicity, and could be used for membrane surface characterization. Gourley et al. (1994) used the sessile drop technique with three probe liquids (water, dimethyl sulfoxide, and α-bromonaphthalene) to characterize the surface energy parameters of UF membranes. Surface energetics were determined for both clean and peptide-fouled membranes. The change in surface energy values due to peptide adsorption was also determined.

2.7 Previous Studies Correlating Contact Angle and Membrane Surface Energetics with Membrane Performance

Several previous studies (e.g., Laîné et al. 1989, Capannelli et al. 1990, Gekas et al. 1992, Gourley et al. 1994, Majewska-Nowak et al. 1997, and Nabe et al. 1997) have been performed on correlating UF contact angle and membrane surface energetics with membrane performance. A few recent investigations (e.g., Kulkarni et al. 1996 and Mukherjee et al. 1996) have been performed on correlating RO membrane contact angle and surface energetics with membrane performance. Additionally, one previous investigation (Sata et al. 1998) evaluated the effect of membrane hydrophobicity on the selectivity of an anion exchange membrane.

Laîné et al. (1989) found relative membrane hydrophobicity to be an important parameter in the performance of UF membranes removing natural organic matter from lake water. The more hydrophobic UF membranes tended to foul at a higher rate than the more hydrophilic membranes. Capannelli et al. (1990) demonstrated that a correlation could be drawn between a UF membrane's relative hydrophobicity and its performance. A higher degree of hydrophilicity resulted in improved membrane flux recovery. Gekas et al. (1992) observed that contact angle hysteresis correlated with UF membrane performance for various solutes, the more hydrophilic the membrane, the higher the relative flux. Contact angle hysteresis was correlated to membrane hydrophobicity, the more hydrophobic a membrane was the more hysteresis was observed. However, it was found that due to the interdependence of contact angle and pore size, contact angle data alone could not be used without consideration of pore size to estimate fouling. Gourley et al. (1994) drew correlations between the total surface energy of several UF membranes varying degrees of hydrophilicity and their performance when subjected to enzymatic hydrolysates. It was found that the hydrophilic membranes

fouled at a lower rate than the more hydrophobic membranes. Majewska-Nowak et al. (1997) investigated the effect of hydrophobicity on the performance of UF membranes used for dye separation. This investigation concluded that hydrophilic membranes are less prone to fouling than hydrophobic membranes. However, in this investigation the relative hydrophilicity of the various UF membranes was based on the hydrophilic properties of the membrane polymers and not on actual membrane measurements. Nabe et al. (1997) used sessile drop and captive bubble contact angle measurements to determine the relative hydrophobicity of several UF membranes. The correlation between membrane hydrophobicity and membrane fouling when exposed to various protein solutions was investigated. This study concluded that the more hydrophilic surfaces experienced less flux-decline than the more hydrophobic surfaces.

Kulkarni et al. (1996) characterized the relative hydrophobicity of hydrophilized thin film composite RO membranes using octane-water contact angle measurements. Decreased hydrophobicity resulted in increased flux and ion rejection. This same conclusion was reached by Mukherjee et al. (1996) during their investigation of thin-film composite RO membranes.

Sata et al. (1998) demonstrated that membrane hydrophobicity affects the permselectivity of an anion exchange membrane. The relative hydrophilicity of an anion exchange membrane was modified using hydrophilic organic compounds and the permselectivity of the membrane in terms of sulfate and chloride ions was examined. It was concluded that membrane ion selectivity was improved by the hydrophilization of the membrane surface.

Investigations performed in the past have shown relationships between a membrane's contact angle or surface energetics and its performance. In all cases, only the "relative" hydrophobicity was determined from contact angle measurements or surface energy parameters. Furthermore, few previous investigations (e.g., Kulkarni et al 1996, Mukherjee et al. 1996, and Sata et al. 1998) evaluated membranes tighter than UF membranes. Studying the hydrophobicity of tighter membranes is important because the fouling mechanisms for looser microfiltration (MF) and UF membranes are substantially different than those for tighter NF and RO membranes.

3 EXPERIMENTAL

3.1 RO and NF Membranes

Four RO membranes and one NF membrane were selected for this investigation. Three of the membranes are cellulose acetate and two are thin-film composite. Table 1 shows the type of membrane, the manufacturer, and the manufacture's flux and rejection data for each of the membranes. All of the membranes are stored in ultrapure water in a refrigerator at 5°C.

Table 1.—Properties of RO and NF membranes selected for this investigation

Membrane	Manufacturer	Type	Average Rejection	Flux[1]	Operating Conditions
FT-30	FilmTec	RO, thin-film composite	99% NaCl	26	2000 ppm NaCl @ 225 psi
CD	Desalination Systems	RO, cellulose acetate	98.5% NaCl	19	2000 ppm NaCl @ 425 psi
CE	Desalination Systems	RO, cellulose acetate	97.5% NaCl	24	2000 ppm NaCl @ 425 psi
CG	Desalination Systems	RO, cellulose acetate	85% NaCl	23	2000 ppm NaCl @ 225 psi
NF-70	FilmTec	NF, thin-film composite	95% $MgSO_4$	Unavailable	2000 ppm $MgSO_4$ @ 70 psi

[1] Flux in gallons per square foot of membrane per day.

3.1.1 Thin Film Composite Membranes

The FT-30 membrane (Film Tec, Minneapolis, MN) is a thin-film composite polyamide membrane. It is a widely used low-pressure RO membrane made by the interfacial polymerization of 1,3-benzenediamine with trimesoyl chloride (Cadotte 1985, Mulder 1991, Petersen 1993, Elimelech et al. 1994, Childress and Elimelech 1996). The NF-70 membrane is a thin-film composite nanofiltration membrane. It is believed to have the same polymeric structure as the FT-30, but has been post-treated with phosphoric acid and tannic acid to open up the pores (Petersen 1993, Childress 1997).

3.1.2 Cellulose Acetate Membranes

Three types of cellulose acetate RO membranes (CD, CE, and CG) were obtained from Desalination Systems (Escondido, California). The three membranes were used to evaluate hydrophobicity and performance differences with membrane of similar chemical compositions. The CD, CE and CG membranes are all heat-treated cellulose triacetate/diacetate blend membranes. The CD and CE are dense

membranes requiring higher operating pressures (~400 psi); the CG is a more swollen membrane that requires lower operating pressures (~225 psi).

3.2 Hydrophobicity Measurements

3.2.1 Automated Goniometer

The automated goniometer used in this investigation is the Rame-Hart (Mountain Lakes, New Jersey) NRL Contact Angle Goniometer. It is a standard goniometer with image analysis attachments (i.e., video camera, computer with monitor, and image analysis software). A photograph of the goniometer apparatus is shown in Figure 5.

Figure 5.—Goniometer apparatus used for contact angle measurements.

The goniometer units (i.e., video camera, light source, and environmental chamber) are built into a metal stand. The stand can be leveled manually with the aid of a leveling bubble and four leveling screws attached to the feet of the stand. This eliminates any slope that may exist in the laboratory test bench that could affect the contact angle measurements. The video camera connects to the computer system through two digital cables. The light source is placed at the opposite end of the video camera. Its intensity is regulated by a control system that is placed on the laboratory bench.

The environmental chamber prevents air movement, dust, and other contaminants from affecting the contact angle measurements or contaminating the probe liquid. The environmental chamber houses a quartz cell, sampling plate, and viewing stage (Figure 6).

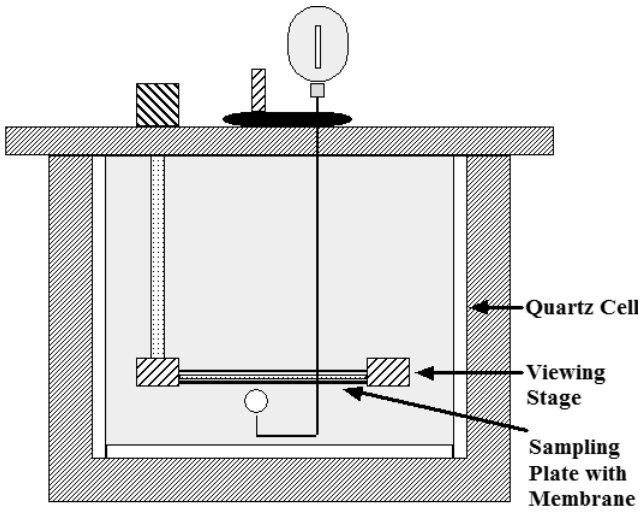

Figure 6.—Environmental chamber for captive bubble measurements.

It is constructed of stainless steel and has glass portals on both sides so that the light source and video camera have access to the sampling plate. The sampling plate and viewing stage are also constructed of stainless steel. The sampling plate is secured to the viewing stage using four screws and two cross bars. The viewing stage is lowered into the quartz cell and secured to the top of the environmental chamber with two steel dowels and two tightening screws. A portal is located on the roof of the environmental chamber to allow for insertion of the needle.

The goniometer uses RH Imaging 2001 software, which has both sessile drop and captive bubble capabilities. The image that appears on the computer screen consists of the membrane being viewed by the camera and several lines that are superimposed by the computer (Figure 7).

These lines designate the region of interest and include a rectangular imaging box, a baseline, and two vertical lines. The rectangular imaging box indicates to the computer the area within which contact angle measurements are taken. The size of the rectangular imaging box must be adjusted as the size of the drop or bubble changes. The size of the box should be minimized to only encompass the area of drop or bubble contact to reduce the chance of inaccurate contact angle readings.

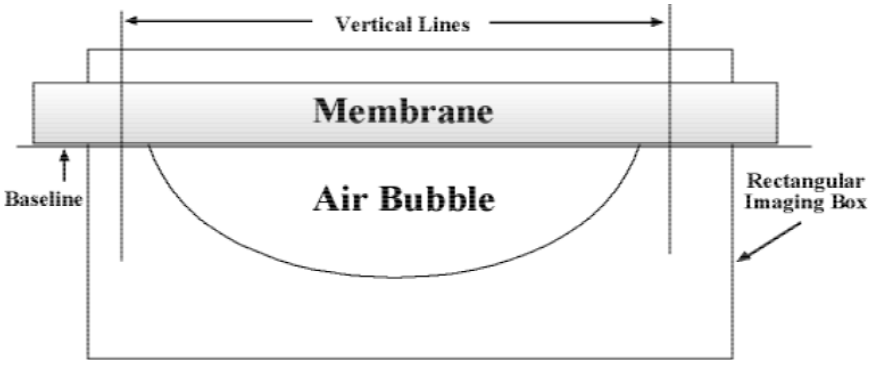

Figure 7.—Computer viewing area with the region of interest designated by the superimposed lines.

As the size of the imaging box increases the possibility of the computer mistaking a surface contaminant for the bubble's point of contact increases. The baseline indicates to the computer where the drop or bubble is contacting the substrate surface and is therefore located at the surface of the substrate. The two vertical lines are gray scale detectors; in other words, they detect the black area (i.e., the substrate) versus the white area (i.e., the probe liquid) of the rectangular imaging box. The two vertical lines must remain half in the black area and half in the white area for proper operation of the imaging software.

To measure contact angles, the computer places a pixel at the point of contact between the bubble and the substrate surface. Using the pixel as the point of origin, the computer draws a line tangent to the boundary of the bubble. The angle between the tangent line and the baseline is calculated as the contact angle. The contact angle is always measured through the denser fluid phase.

3.2.2 Syringe and U-Shaped Needle

Air bubbles are delivered to the membrane surface using a 20-µL syringe (Hamilton Instruments, Reno, Nevada). The syringe is capable of delivering precise volumes of air (within 0.01 µL) using a built-in volume selection and locking mechanism. The ability of the syringe to deliver precise volumes of air reduces errors associated with varying bubble volumes. A bent U-shaped needle is attached to the syringe in order to deliver air bubbles to the underside of the membrane coupon in the environmental chamber.

The needle and syringe are cleaned prior to each set of contact angle measurements. The cleaning procedure utilizes three solvents: ultrapure water, hexane, and acetone. The ultrapure water removes any water-soluble contaminants. The acetone removes any polar but non-water soluble contaminants. The hexane removes any non-polar contaminants. The syringe is cleaned by the following cycle: water, acetone, hexane, water, acetone, hexane, water, water.

3.2.3 Probe Liquids

Calculation of the hydrophobicity of a membrane sample requires three probe liquids with well-known surface tension properties (van Oss 1993). The probe liquids selected for this investigation are glycerol (polar), ultrapure water (polar), and diiodomethane (apolar). These probe liquids were chosen on the premise that two must be polar and one must be apolar. The glycerol and diiodomethane were obtained from Fisher Scientific (Pittsburgh, PA). Ultrapure water was obtained from a Millipore (Burlington, MA) water purification system. Each liquid has three surface tension parameters, γ^{LW}, γ^{+}, and γ^{-}. These parameters as well as the polar energy component, γ^{AB} and the total free energy component, γ_l are found in Table 2.

Table 2.—Surface tension properties (mJ/m²) of probe liquids at 20 °C (as taken from van Oss, 1993)

Liquid	γ_l^{LW}	γ_l^+	γ_l^-	γ_l^{AB}	γ_l^{TOT}
Diiodomethane	50.8	0.0	0.0	0.0	50.8
Ultrapure water	21.8	25.5	25.5	51.0	72.8
Glycerol	34.0	3.9	57.4	30.0	64.0

As seen in Table 2, the γ^+ and γ^- (and therefore γ^{AB}) parameters for the diiodomethane are zero because in purely apolar systems only LW forces operate. Also from Table 2, the γ^+ and γ^- parameters for water are shown to be equal. The value for the two water parameters is based on the following relationship:

$$\gamma_l^+ = \gamma_l^- = \frac{1}{2} \times 51 \frac{mJ}{m^2} = 25.5 \frac{mJ}{m^2} \tag{18}$$

where 51 mJ/m^2 is the value of γ^{AB} for water (van Oss 1993).

3.2.4 Bubble Volume

Bubble volume directly affects the contact angle of a liquid on a solid surface (Good and Koo 1979, Drelich and Miller 1994). As bubble volume increases the contact angle reaches a temporary state of equilibrium with the solid surface (Drelich et al. 1996). The temporary state of equilibrium reached will change based on the amount of available external energy available for overcoming existing energy barriers, such as vibrations or an increase in bubble volume (Drelich et al. 1996). Therefore, a constant bubble volume must be used in order to obtain reproducible contact angle results. A 10-µL bubble was selected for this investigation to provide a bubble of significant size so as to make its edges clearly visible.

3.2.5 Parafilm® Standard

Contact angle measurements were performed on commercially available Parafilm® (Fisher Scientific, Pittsburgh, PA) using the captive bubble method. The results were then compared to values from the literature (e.g., Busscher et al. 1983, Dann 1970, Zhang and Hallström 1990) (Table 3). Measurements performed over a 3-day period resulted in an average contact angle of 110±1°. As can be seen from Table 3, results from this investigation are in complete agreement with those in the literature.

Table 3.—Comparison of contact angle measurements for water on Parafilm®

Current Investigation[1]	Dann (1970)[2]	Busscher et al. (1983)[1]	Zhang and Hallström (1990)[1]
110 ± 1°	110 ± 2°	108 ± 2°	108 ± 3°

[1] Contact angles were measured using the captive bubble technique.
[2] Contact angles were measured using the sessile drop technique.

3.2.6 Contact Angle Measurement Procedure

The procedure used to measure the captive bubble contact angle is outlined below. It should be noted that the set-up of the goniometer and cleaning of the micro-syringe discussed earlier were also part of the procedure.

1. A membrane coupon having the approximate dimensions 1.0 × 0.25 inches was cut from the membrane sample which was stored in ultrapure water at 5 °C.
2. The membrane coupon was wrapped around the sampling plate and secured on the viewing stage. The viewing stage was lowered into the probe liquid contained in the quartz cell and the environmental chamber was sealed. The leveling and lighting conditions of the viewing area were checked using the imaging software.
3. A 10-µL air bubble was released from the U-shaped needle into the quartz cell containing the probe liquid. The bubble floated approximately 0.4 inch to the membrane surface held by the viewing stage.
4. The goniometer's video camera was focused on the air bubble.
5. Two contact angle measurements (one on each side of the bubble) were taken at time zero and then at 5-min intervals over the next 20 min.

The data presented in Figure 8 demonstrates that in the captive bubble method, the average contact angle is relatively independent of time (for up to 50 min).

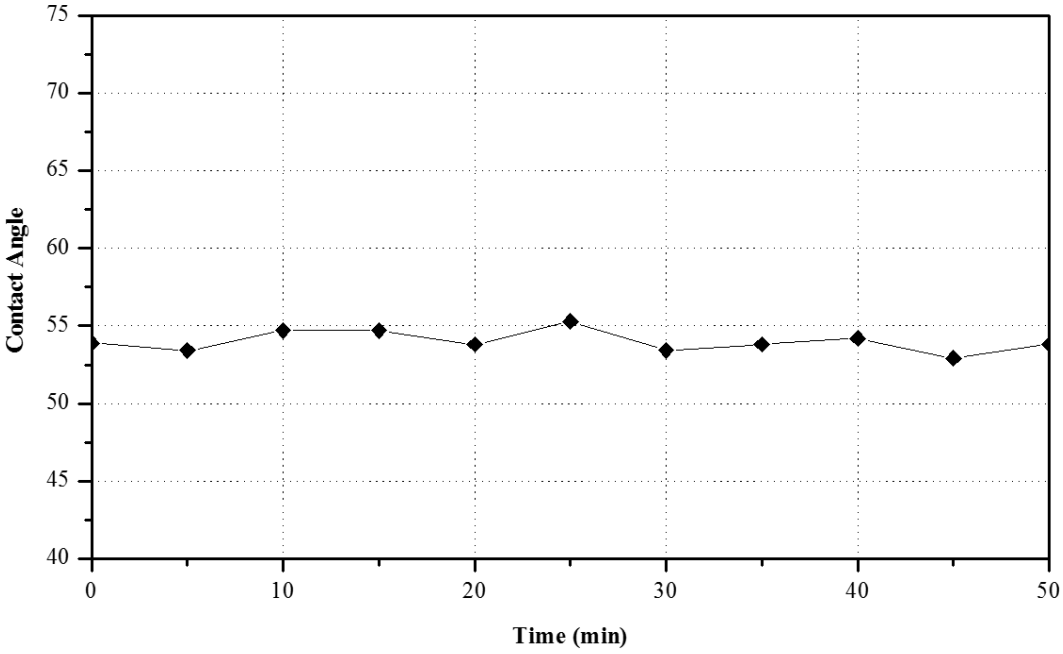

Figure 8.—Contact angle for CE membrane in ultrapure water as a function of time.

This was found to hold true for all membrane/probe liquid combinations. Contact angles were expected to be independent of time because of the complete membrane saturation that prevents infiltration of the air bubble into the pores of the membrane (Dahlgren et al. 1986).

Because the membranes and test liquids have unique characteristics, some modifications to the measurement procedure were required for the different membrane/probe liquid combinations. These modifications were determined from preliminary contact angle measurements and are discussed in the following paragraphs. The CE membrane was selected for preliminary contact angle measurements as a representative of the three cellulose acetate membranes used in this study. Data for all membrane/probe liquid combinations is reported at the 15-min measurement interval. The 15-min measurement interval was selected because it provides a more than adequate equilibration period.

3.2.7 Preliminary Contact Angle Measurements for Ultrapure Water

The primary obstacle encountered when using the ultrapure water was the rolling of air bubbles off some of the membrane surfaces. This problem was rectified by increasing the travel distance of the air bubble to the membrane surface from 0.2 to 0.4 inches. By increasing the travel distance, approximately three out of four air bubbles attached to the membrane surface in repeated trials (75% attachment efficiency). The increased attachment efficiency is attributed to the decrease in the impact velocity of the air bubble to the membrane surface.

Preliminary contact angle measurements performed on the CE membrane coupon immersed in ultrapure water had a significantly large standard deviation (10.2°). The average standard deviation for contact angle measurements to be considered accurate is ~ 2° (Zhang and Hallström 1990), making a standard deviation of 10.2° very high. Upon close inspection, the surface of the CE membrane was observed to be contaminated with cardboard particulates. The particulates were believed to have come from the shipping container (a cardboard tube). Although the CE membrane had been thoroughly rinsed with ultrapure water, it appears that not all of the particulates were removed. As all three cellulose acetate membranes were shipped in the same container, all three were believed to have been affected in the same way. Therefore, to minimize the amount of particulate matter on the cellulose acetate membrane surfaces, additional rinses were done on these membranes. Following the additional rinses, the preliminary contact angle measurements were repeated on the CE membrane. These results had a standard deviation of 2.0°.

Contact angle measurements performed on the FT-30 and NF-70 membrane coupons produced results with a standard deviation of 1.0° and 2.0°, respectively. Surface contamination was not an issue with either membrane, and thus contact angle measurements were highly reproducible.

3.2.8 Preliminary Contact Angle Measurements for Glycerol

In performing contact angle measurements on the membrane coupons using the glycerol probe liquid, it was observed that as the viewing platform was lowered into the glycerol a type of “smear zone” was formed. The smear zone actually consisted of entrapped air. The smear zone prevented the goniometer from focusing on the air bubble on the membrane surface. It also temporarily prevented the formation of a clear interface between the membrane surface and the air bubble and resulted in widely varying contact angles. It was found that if the viewing platform and the membrane sample were left in the glycerol for a period of 24 hours the smear zone disappeared and a clear interface developed between the membrane surface and the glycerol. The air-tight environmental chamber prevented contamination of the glycerol over the 24-hour period. Following this adjustment to the test procedure, reproducible contact angle measurements were obtained for each of the three membrane coupons using the glycerol probe liquid.

Contact angle measurements for the CE, FT-30, and NF-70 membrane coupons immersed in the glycerol probe liquid had standard deviations of 2.1°, 2.5°, and 1.0°, respectively. The low standard deviation is attributed to the stability of the air bubble in the glycerol. Because glycerol has a low viscosity, the air bubble is extremely stable on the surface of the membrane. The glycerol has a much lower tendency than the ultrapure water to allow for bubble movement. Therefore, the air bubble is resistant to even the slightest movement that would cause a deviation in contact angle measurements over time.

3.2.9 Preliminary Contact Angle Measurements for Diiodomethane

Preliminary contact angle measurements on the membranes using the diiodo methane probe liquid showed that the test procedure required no adjustments. Contact angle measurements for the CE, FT-30, and NF-70 membrane coupons immersed in the diiodomethane probe liquid had standard deviations of 1.0°, 1.3°, and 2.2°, respectively.

3.3 Membrane Performance Tests

3.3.1 Membrane Test Unit

The membrane test unit was a bench-scale RO/NF system with partially automated data acquisition. In-line computer interfaced digital probes (Omega Engineering, Stamford, Connecticut) were used to measure temperature, pH, conductivity, flowrate, and pressure. Data was acquired and displayed by LabVIEW data acquisition software (National Instruments, Austin, Texas). LabVIEW uses the probes as virtual instruments that may be controlled and viewed by the computer.

A schematic of the membrane test unit is shown in Figure 9. The test solution was held in a 5.5-gallon Plexiglas reservoir (Cole-Parmer, Vernon Hills, IL). The temperature in the reservoir was kept constant (25 °C) using a cooling coil and a refrigerated recirculating chiller (Cole Parmer, Vernon Hills, IL). The test solution was fed to two parallel flat sheet membrane test cells (Industrial Research Machine Products Co., Los Angeles, CA) using a positive displacement pump (CAT Model 280, Aries Supply and Equipment, North Hollywood, CA) capable of providing hydraulic pressures up to 1,000 psi and a maximum flowrate of 3.0 gpm. The two membrane test cells operated at a constant crossflow velocity of 0.5 gpm for all trials. The test cells contained flat sheet membrane coupons with dimensions of 1.0 × 3.0 inches. The cross-flow velocity across the membrane cells was controlled using a bypass valve (Oakland Valve and Fittings, Concord, CA). Both the permeate and concentrate were recycled to the reservoir. Pressure across the membrane cells was controlled using a back-pressure regulator (Oakland Valve and Fittings, Concord, CA).

Feed solution conductivity, pH, and temperature were measured using computer-interfaced digital probes in the reservoir. System pressure was measured using a computer-interfaced in-line sensor located on the effluent line from the pump. Cross flow velocity was monitored using an in-line flow meter (Cole-Parmer, Vernon Hills, IL) on the common concentrate line. Permeate flux was measured using a graduated cylinder and stopwatch, salt rejection was measured using a conductivity meter (CDTX820 series, Omega Engineering, Inc., Stamford, CT), and permeate pH was measured using a pH meter (PHTX820 series, Omega Engineering, Inc., Stamford, CT).

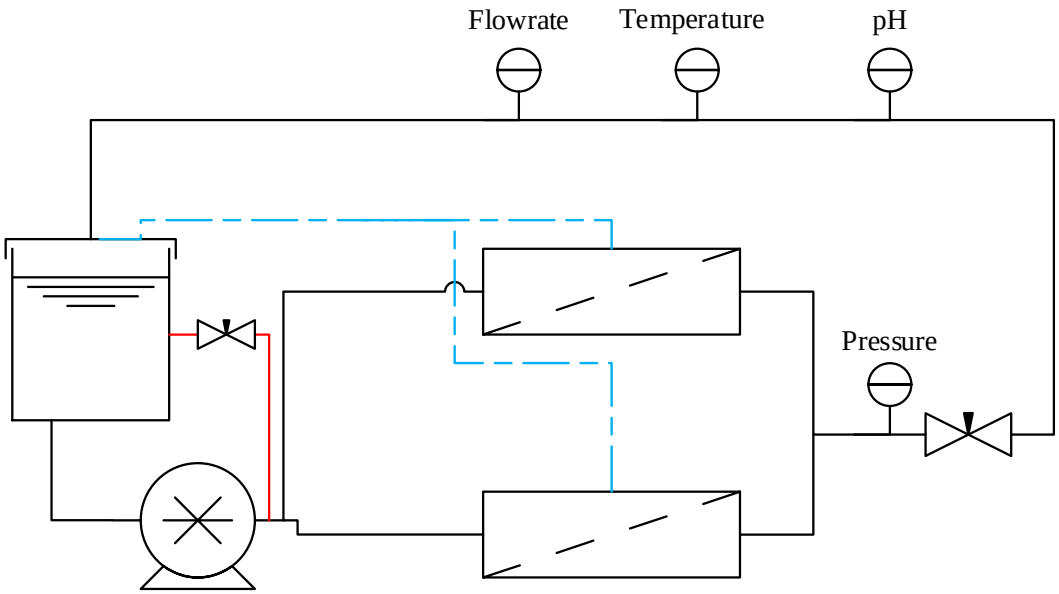

Figure 9.—A schematic of the membrane test unit.

3.3.2 Solution Chemistries

Three test solutions were used in the membrane performance test:

1) 0.01 *M* NaCl
2) 1 *mM* sodium dodecyl sulfate plus 0.01 *M* NaCl
3) 10 mg/L peat humic acid plus 1 *mM* $CaCl_2$ plus 0.01 *M* NaCl.

The 0.01 *M* NaCl run is used for the baseline. Then, 0.01 *M* NaCl is used as a background electrolyte for the humic and surfactant runs.

Certified ACS grade sodium chloride (NaCl) (Fisher Scientific, Pittsburgh, PA) was used in all runs. Certified ACS grade calcium chloride ($CaCl_2$) (Fisher Scientific, Pittsburgh, PA) was used in the peat humic acid runs. Certified grade sodium hydroxide (NaOH) (Fisher Scientific, Pittsburgh, PA) was used for preparing the humic stock solution.

Peat humic acid (PHA) was acquired from the International Humic Substance Society (St. Paul, MN) in a freeze-dried form. A stock solution (1.0 g/L) was prepared by dissolving the humics in ultrapure water and raising the pH to 8.0 with NaOH. The reported molecular weight for PHA ranges from 10,000 to 30,000 daltons (Hong and Elimelech 1997). Hong and Elimelech (1997) found PHA to have a carboxylic acidity of 3.7 milliequivalents per gram, which is slightly lower than the value (4.8 milliequivalents per gram) found by Amirbahman and Olson (1995).

Certified grade sodium dodecyl sulfate (Fisher Scientific, Pittsburgh, PA) was used as a model anionic surfactant. The surfactant concentration used was 1 *mM*. This concentration was slightly below the corresponding critical micelle concentration of approximately 3.16 *mM* (in the presence of 0.01 *M* NaCl) (Mukerjee and Mysels 1970).

3.3.3 Performance Test Protocol

Prior to the performance test, the membrane coupons were rinsed in a flow through mode with 5.5 gallons of ultrapure water to remove impurities that may be attached to the membrane surface. The membranes were then equilibrated under normal operating pressure for approximately 45 hours with 0.01 *M* NaCl solution. Following this period, the permeate flux and salt rejection was found to be constant or the experiment was discontinued. For the humic and surfactant runs, the humic or surfactant was added immediately after the equilibration period.

Membrane performance tests were conducted for a period of approximately 1 hour after the 45-hour equilibration period. Membrane performance was evaluated at pH ~ 5.6. The flux and rejection of each membrane was monitored at 10-min intervals over a 60-min time span. A 60-min observation period was sufficient to analyze the interaction between the foulant and the membrane surface. After 60 min the foulant may no longer be interacting with the membrane surface, but instead may be interacting with the foulant layer forming on the membrane surface. A foulant or cake layer generally occurs on the order of minutes or hours following the introduction of the foulant to the feed stream (Song and Elimelech 1995b).

3.3.4 Performance Analysis

The effect of the humic or surfactant on membrane performance was quantified using flux and rejection ratios. Flux and rejection ratios provide a method for comparing changes in flux and rejection for membranes that have a wide range of initial flux or rejection values. The flux ratio is a ratio of the water flux at time *t* to the original water flux prior to the addition of the foulant. The flux ratio was calculated using the following equation:

$$J_i = \frac{j_i}{j_o} \tag{19}$$

where J_i is the flux ratio at time *t*
j_i is the water flux at time *t*
j_o is the original water flux prior to addition of the foulant

The times evaluated in this investigation were 5 min, 20 min, 35 min, and 50 min after the addition of the foulant. These times correspond to j_5, j_{20}, j_{35}, and j_{50} in Figure 10.

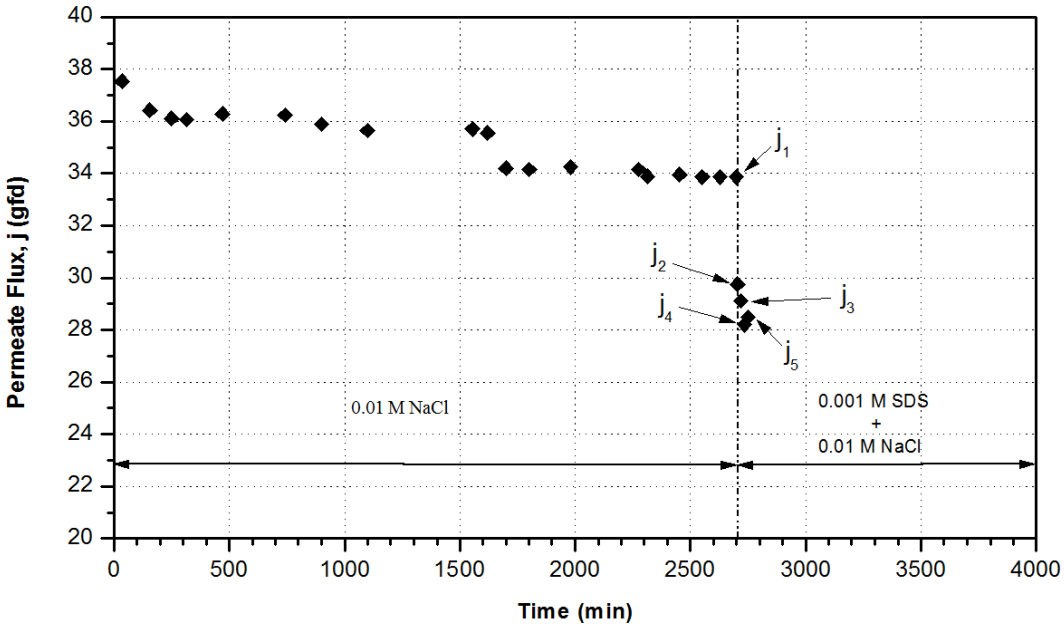

Figure 10.—Permeate flux and rejection measurement points for calculating flux and rejection ratios.

Similarly, rejection ratios were calculated at 5 min, 20 min, 35 min, and 50 min using the equation:

$$R_i = \frac{r_i}{r_o} \tag{20}$$

where R_i is the rejection ratio at time t
r_i is the salt rejection at time t
r_o is the original salt rejection prior to addition of the foulant

4 RESULTS AND DISCUSSION

4.1 Hydrophobicity of Clean Membrane Coupons

Contact angle measurements performed on the five membrane coupons (FT-30, CD, CE, CG, and NF-70) using the three probe liquids (ultrapure water, glycerol, and diiodo methane) produced the results shown in Table 4. Values found in Table 4 represent the mean of at least 18 air bubbles, and are reported with their respective 95% confidence limits.

Table 4.—Average contact angle measurements and 95% confidence limits for clean membrane coupons

Coupon	Ultrapure water	Glycerol	Diiodomethane
FT-30	52.7° ± 0.7°	46.1° ± 1.1°	55.9° ± 1.7°
CD	48.4° ± 1.5°	42.5° ± 1.1°	53.5° ± 2.2°
CE	52.8° ± 0.8°	51.3° ± 0.9°	54.4° ± 1.3°
CG	60.2° ± 1.2°	55.4° ± 0.5°	59.1° ± 0.9°
NF-70	39.8° ± 1.7°	37.4° ± 0.7°	52.5° ± 1.9°

The results for each membrane/probe liquid combination were substituted into equation 16.

$$(1+\cos\theta)\gamma_l^{TOT} = 2\left(\sqrt{\gamma_s^{LW}\gamma_l^{LW}} + \sqrt{\gamma_s^{+}\gamma_l^{-}} + \sqrt{\gamma_s^{-}\gamma_l^{+}}\right) \quad (16)$$

This resulted in three equations with three unknowns (γ_s^{LW}, γ_s^{+}, and γ_s^{-}) for each membrane. The three equations were solved simultaneously to determine the three surface tension parameters of each membrane (Table 5).

Table 5.—Surface tension properties (mJ/m^2) for clean membrane coupons

Coupon	γ_s^{LW}	γ_s^{+}	γ_s^{-}	γ_s^{AB}	γ_s
FT-30	30.9	2.6	23.3	15.6	46.5
CD	32.3	2.7	26.1	16.8	48.9
CE	31.8	1.4	26.9	12.3	43.9
CG	29.1	1.7	20.4	11.8	40.8
NF-70	32.9	2.7	33.6	19.0	52.0

These three parameters along with the surface tension parameters for ultrapure water were then substituted into equation 17.

$$\Delta G_{sl} = -2\left(\sqrt{\gamma_s^{LW}} - \sqrt{\gamma_l^{LW}}\right)^2 - 4\sqrt{\gamma_s^+\gamma_s^-} + \sqrt{\gamma_l^+\gamma_l^-} - \sqrt{\gamma_s^+\gamma_l^-} - \sqrt{\gamma_s^-\gamma_l^+} \quad (17)$$

This resulted in an exact determination of the free energy of hydrophobic interaction for each membrane with water (Table 6).

Table 6.—Free energy of hydrophobic interaction (mJ/m^2) for clean membrane coupons in ultrapure water

Coupon	ΔG_{SW} (mJ/m^2)	Hydrophobicity
FT-30	–4.72	Hydrophobic
CD	–1.22	Slightly hydrophobic
CE	0.18	Slightly hydrophilic
CG	–9.14	Hydrophobic
NF-70	7.82	Hydrophilic

4.1.1 Sample Calculation

A sample calculation for the CE membrane coupon is shown below using the average contact angle data from Table 4 and the surface energy properties of the probe liquids from Table 3.

1. For ultrapure water

$$\left(1+\cos 52.8^\circ\right)72.8 = 2\left[\sqrt{\gamma_S{}^{LW} * 21.8} + \sqrt{\gamma_S{}^{+} * 25.5} + \sqrt{\gamma_S{}^{-} * 25.5}\right]$$

2. For glycerol

$$\left(1+\cos 51.3^\circ\right)64.0 = 2\left[\sqrt{\gamma_S{}^{LW} * 34.0} + \sqrt{\gamma_S{}^{+} * 3.9} + \sqrt{\gamma_S{}^{-} * 57.4}\right]$$

3. For diiodomethane

$$\left(1+\cos 54.4^\circ\right)50.8 = 2\sqrt{\gamma_S{}^{LW} * 50.8}$$

These three equations are solved for the three unknown surface tension parameters. The surface tension parameters for the CE membrane (Table 5) are:

$\gamma_s^{LW} = 31.8$ mJ/m^2
$\gamma_s^{+} = 1.4$ mJ/m^2
$\gamma_s^{-} = 26.9$ mJ/m^2

These parameters, along with the surface tension parameters for ultrapure water, were substituted into equation 17 in order to calculate the free energy of hydrophobic interaction with water (Table 6).

$$\Delta G_{sw} = -2\left(31.8 - 21.8\right)^2 - 4\left(\sqrt{1.4 * 26.9} + \sqrt{25.5 * 25.5} - \sqrt{1.4 * 25.5} - \sqrt{26.9 * 25.5}\right)$$
$$\Delta G_{SW} = 0.18\ mJ\ /\ m^2$$

Similar calculations were performed for the FT-30, CD, CG, and NF-70 membranes.

The results (Table 6) indicated that the NF-70 membrane was the most hydrophilic (ΔG_{SW} = 7.82 mJ/m^2) and the CG membrane was the most hydrophobic (ΔG_{SW} = –9.14 mJ/m^2). The FT-30 and CD membranes have hydrophobic tendencies (ΔG_{SW} = –4.72 and –1.22 mJ/m^2, respectively). Results for the CE membrane (ΔG_{SW} = 0.18 mJ/m^2) indicated insignificant hydrophilic tendencies. With the exception of the CE membrane, hydrophobicity decreased with increasing pore size. This observation agreed with Gekas et al. (1992), who observed that more porous membranes had a lower apparent hydrophobicity. However, further investigation is warranted as other investigations (e.g., Oldani and Schock 1989, Capannelli et al. 1990, Jucker and Clark 1994, and Nabe et al. 1997) have found the opposite trend to be true.

All five membranes have high electron-donor monopolarity; in other words, they have relatively high electron-donor components (γ^-) and relatively low electron-acceptor components (γ^+) (Table 5). High electron-donor monopolarity has previously been reported for polysulfone and polyethersulfone UF membranes (Gourley et al. 1994) and for polyamide NF membranes (Bouchard et al. 1997). Also from Table 5, all of the membranes investigated have predominately nonpolar (LW) surfaces. In all cases, the nonpolar (LW) contribution was approximately twice that of the polar (AB) contribution. The NF-70 membrane had the highest AB contribution (19.0 mJ/m^2), while the CG membrane had the lowest (11.8 mJ/m^2). Higher values of γ^{AB} are characteristic of hydrophilic surfaces (van Oss et al. 1986b). Therefore, based on values of γ^{AB}, the NF-70 would be the most hydrophilic and the CG would be the most hydrophobic. These results agree with the free energy of hydrophobic interaction (ΔG) calculations (Table 6), which prove the NF-70 membrane to be the most hydrophilic and the CG membrane to be the most hydrophobic.

4.2 Membrane Performance Trials

Flux and rejection ratios for the surfactant and humic acid performance trials are presented in Tables 7 and 8. Following the addition of the surfactant to the feed stream, the FT-30 and NF-70 membranes experienced substantially greater flux decline than the CD, CE, and CG membranes. Over the entire 60-min test period, the cellulose acetate membranes were less affected by surfactant adsorption than the thin-film composite membranes. The same was true for the humic acid performance trials.

Table 7.—Performance results for surfactant fouling experiments

Membrane	ΔG_{SW}	J_5	J_{20}	J_{35}	J_{50}	R_5	R_{20}	R_{35}	R_{50}
FT-30	–4.72	0.88	0.86	0.83	0.84	1.00	1.05	1.05	1.05
CD	–1.22	0.96	1.00	1.01	1.00	1.01	1.03	1.04	1.04
CE	0.18	0.96	0.96	0.92	0.94	1.02	1.05	1.06	1.06
CG	–9.14	0.92	0.93	0.91	0.92	1.12	1.15	1.15	1.15
NF-70	7.82	0.90	0.87	0.85	0.85	1.06	1.11	1.12	1.12

Table 8.—Performance results for humic acid fouling experiments

Membrane	ΔG_{SW}	J_5	J_{20}	J_{35}	J_{50}	R_5	R_{20}	R_{35}	R_{50}
FT-30	–4.72	0.91	0.90	0.89	0.88	1.02	1.00	1.00	1.00
CD	–1.22	0.97	0.97	0.97	0.97	1.03	1.02	1.02	1.01
CE	0.18	0.97	0.98	0.99	0.99	1.05	1.02	1.02	1.02
CG	–9.14	0.98	0.95	0.97	0.97	1.17	1.03	1.02	1.01
NF-70	7.82	0.86	0.84	0.80	0.78	1.08	0.97	0.97	0.98

Rejection ratios for the surfactant and humic acid performance trials did not follow the same trend as the flux ratios. Rejection ratios were not substantially different when comparing the thin-film composite and cellulose acetate membranes. For both the cellulose acetate and thin-film composite membranes, rejection ratios increased immediately following the addition of the surfactant or humic acid to the feed stream. However, it is interesting to note that for the surfactant performance trials, rejection ratios increased over the 60-min observation period for all membranes tested. On the other hand, for the humic acid trials, rejection ratios, decreased over the 60-min observation period for all membranes during the humic acid performance trials. In order to understand the true nature of these rejection ratio trends, longer performance trials would be required.

4.3 Surface Energetics of Membranes Following Surfactant and Humic Performance Experiments

Contact angle measurements (n = 9) were performed on all membrane coupons following the completion of the surfactant and humic acid performance experiments. Contact angle data for the used membrane coupons are found in Table 9. Contact angle measurements for the used membranes possessed 95% confidence limits ranging from 0.5° to 11.0°. The large range of the confidence limits prevented the conclusive determination of the actual contact angle for the used membranes. Due to the uncertainty of the contact angles, calculation of the surface energetics and free energies was not pursued.

Table 9.—Average contact angle measurements and 95% confidence limits for used membrane coupons

Membrane coupon	Solution chemistry*	Ultrapure water	Glycerol	Diiodomethane
FT-30	SDS	51.4° ± 1.6°	36.9° ±11.4°	66.9° ± 9.2°
CD	SDS	29.6° ± 4.8°	41.2° ± 2.8°	55.7° ± 4.8°
CE	SDS	36.0° ±10.2°	43.3° ± 0.5°	70.9° ±10.8°
CG	SDS	42.2° ± 1.5°	36.9° ± 3.3°	82.4° ± 6.2°
NF-70	SDS	47.3° ± 6.5°	38.8° ± 8.2°	72.0° ± 2.7°
FT-30	PHA + $CaCl_2$	48.8° ± 2.0°	48.0° ± 3.5°	64.9° ± 3.7°
CD	PHA + $CaCl_2$	35.9° ±10.5°	51.5° ± 7.9°	58.9° ± 3.6°
CE	PHA + $CaCl_2$	32.2° ± 8.4°	43.3° ± 5.8°	61.9° ± 2.0°
CG	PHA + $CaCl_2$	44.9° ± 6.4°	43.5° ± 5.8°	61.5° ± 5.3°
NF-70	PHA + $CaCl_2$	48.6° ± 3.1°	36.3° ± 2.5°	66.4° ± 6.1°

* All solution chemistries have a background electrolyte of 0.01 *M* NaCl.

4.4 Hydrophobicity Versus Contact Angle with Water

In previous investigations (e.g., Laîné et al. 1989, Capannelli et al. 1990, Gekas et al. 1992, Gourley et al. 1994, Majewska-Nowak et al. 1997, and Nabe et al. 1997), contact angle measurements with water have been used to gain insight into membrane hydrophobicity instead of calculated hydrophobicity values, partially because contact angle measurements are easier to perform. However, there is some question as to whether or not contact angle measurements are an adequate

surrogate for hydrophobicity measurements. Table 10 compares results for hydrophobicity and contact angle with water.

Table 10.—Comparison of hydrophobicity and contact angle results

Membrane	ΔG_{sw} (mJ/m^2)	Hydrophobicity	Contact angle with water	Hydrophobicity
FT-30	–4.72	Hydrophobic	52.7°	Slightly hydrophobic
CD	–1.22	Slightly hydrophobic	48.4°	Slightly hydrophilic
CE	0.18	Slightly hydrophilic	52.8°	Slightly hydrophobic
CG	–9.14	Hydrophobic	60.2°	Hydrophobic
NF-70	7.82	Hydrophilic	39.8°	Hydrophilic

Contact angle results agreed with calculated values for the two most extreme cases: the most hydrophilic membrane (the NF-70 membrane) and the most hydrophobic membrane (the CG membrane). However, contact angle results for the membranes that show less distinct hydrophobic/hydrophilic tendencies (the FT-30, CD, and CE membranes) do not exactly agree with the calculated values for hydrophobicity. According to the contact angle results, the FT-30 and CE membranes should be more hydrophobic than the CD membrane. However, the hydrophobicity results show that the FT-30 membrane is more hydrophobic than the CD membrane which is more hydrophobic than the CE membrane. Therefore, it can be concluded that contact angle measurements are adequate for making hydrophobicity/hydrophilicity generalizations, but may not be accurate when differences in hydrophobicity/hydrophilicity are more subtle. Additionally, with contact angle measurements alone, there is no clear distinction between hydrophobic and hydrophilic membranes. In comparing the hydrophobicity and contact angle results, the dividing line between hydrophobicity and hydrophilicity occurs at a contact angle around 50°. If just evaluating the contact angle data alone, the dividing line between hydrophobicity and hydrophilicity could not be determined.

4.5 Role of Membrane Hydrophobicity in Membrane Flux Decline

Table 11 compares three membrane properties with flux decline for the surfactant and humic acid experiments. Porosity is based on manufacturer's rejection data. Roughness is based on a previous investigation (Childress 1997). In general, thin-film composite NF membranes have been found to be more smooth than thin-film composite RO membranes. Also, cellulose acetate membranes have been found to be more smooth than thin-film composite membranes (Elimelech et al. 1997 and Childress 1997). From Table 11, the more hydrophobic, porous, and rough membranes are expected to result in greater flux decline than the more hydrophilic,

tight, and smooth membranes. Basically, more porous membranes may suffer from pore blockage (Zhang and Hallström 1990) which may result in greater flux decline than less porous membranes. Additionally, increased surface roughness has been found to result in increased flux decline (Elimelech et al. 1997).

Table 11.—Flux decline as a function of three membrane properties

Flux decline	Hydro-phobicity	Porosity	Roughness	Flux decline (surfactant)	Flux decline (humic acid)
High	CG	NF-70	FT-30	FT-30	NF-70
↓	FT-30	CG	NF-70*	NF-70	FT-30
↓	CD	CE	CG, CD, CE**	CG	CG, CD
↓	CE	CD		CD, CE	CE
Low	NF-70	FT-30			

* Based on atomic force microscope measurements on a similar membrane (NF-55 membrane, Film Tec, Minneapolis, Minnesota) (Childress 1997).
** Based on atomic force microscope measurements on the CG membrane only (Childress 1997).

Based on the data in Table 11, it appears that surface roughness is the controlling factor for flux decline for both the surfactant and humic acid performance trials. In both the surfactant and humic acid performance experiments, the rougher thin-film composite membranes have greater flux decline than the smoother cellulose acetate membranes. From this observation it seems prudent to separate the membranes into two groups for comparison: thin-film composite membranes and cellulose acetate membranes. By separating the membranes into two groups it is possible to analyze membranes that are more similar in construction in order to make further observations. The secondary controlling factor for the thin-film composite membranes in the surfactant experiments is likely to be surface roughness and/or hydrophobicity. For the cellulose acetate membranes in the surfactant experiments, roughness, porosity, and/or hydrophobicity are all possible as secondary controlling factors. In the humic performance experiments, the secondary controlling factor is likely to be membrane porosity for the thin-film composite membranes, and roughness and/or hydrophobicity for the cellulose acetate membranes.

4.6 Correlations between Membrane Hydrophobicity and Membrane Performance

Hydrophobicity appears to be a secondary controlling factor in flux decline. Further investigation to determine how much of a role hydrophobicity plays in flux decline would require analysis of membranes with similar surface roughness and porosity. As the goal of this investigation was to evaluate commercial RO and NF membranes, differences in roughness and porosity are difficult to rule out.

Therefore in looking at significant correlations between membrane hydrophobicity and membrane performance the membranes were evaluated in two subsets of three membranes each. The most selective membranes (FT-30, CD, and CE membranes) were evaluated first. Leaving the NF-70 and CG membranes out of this set was justified because of their substantially lower salt rejection (70% and 85% respectively, as compared to > 97%). Then, the cellulose acetate membranes (CD, CE, and CG membranes) were evaluated. Removing the NF-70 and FT-30 membranes from this subset was justified because although the three cellulose acetate membranes have slightly different chemical compositions, they are still composed of the same class of polymers. Therefore, in further analysis, the membranes have been separated into two subsets: the most selective membranes (the FT-30, CD, and CE membranes) and the cellulose acetate membranes (the CG, CD, and CE membranes).

In analyzing the performance data for correlations between membrane hydrophobicity and flux decline, j_5, j_{20}, j_{35}, and j_{50} data was used. However, correlations with membrane hydrophobicity were only found to exist for the j_5 and j_{20} data (except in one case). At 5 and 20 minutes it is not likely that the foulant has formed a secondary layer (or cake layer) on the membrane; in other words, it is likely that the foulant is still encountering and reacting with the membrane surface itself.

Correlations of J_5 with ΔG_{sw} for the most selective membrane subset and cellulose acetate membrane subset are shown in Figures 11 and 12, respectively.

In both cases, fouling increases with increasing hydrophobicity (decreasing interfacial free energy). As time progressed beyond the first measurement interval at 5 min, no significant ($R^2 > 0.80$) correlations could be drawn.

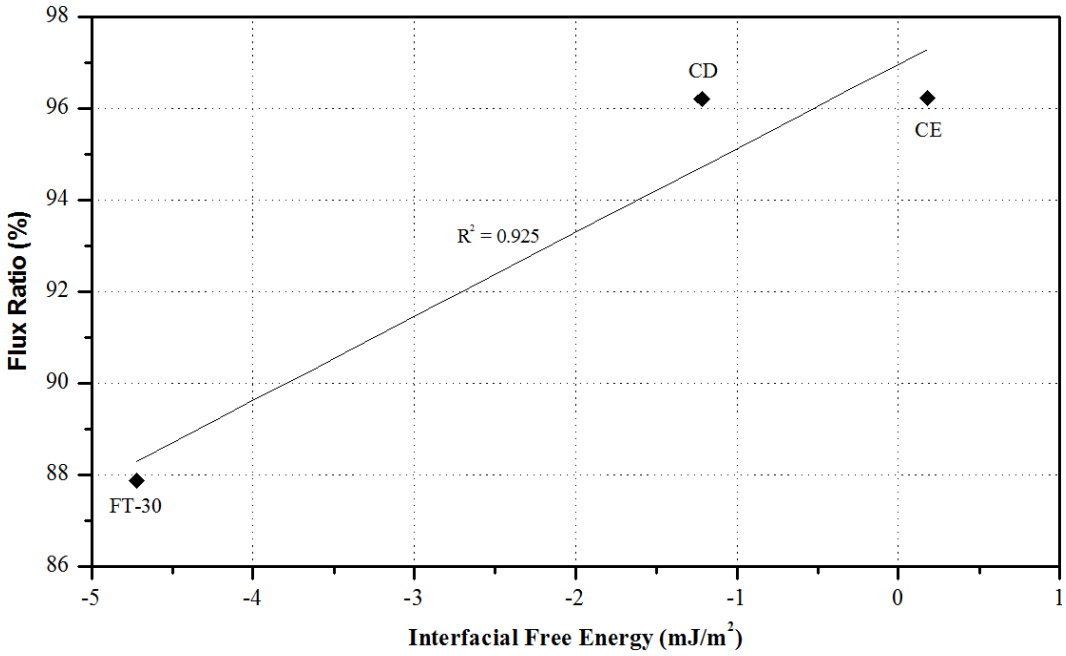

Figure 11.—Flux ratio at 5 minutes as a function of interfacial free energy for the most selective membrane subset during SDS performance trials.

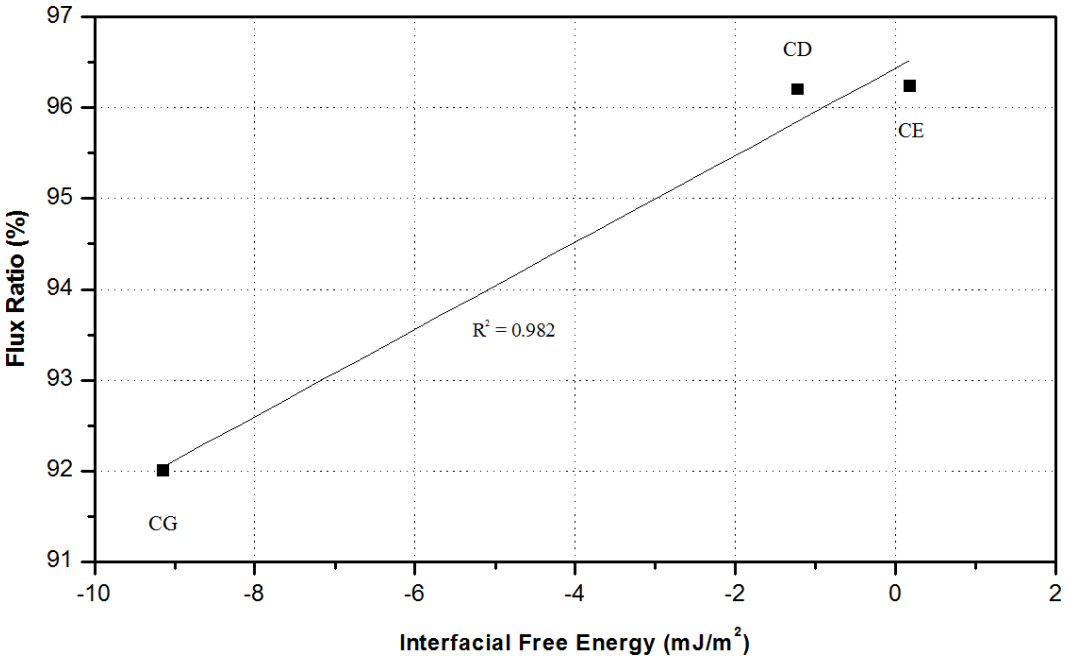

Figure 12.—Flux ratio at 5 minutes as a function of interfacial free energy for the cellulose acetate membrane subset during SDS performance trials.

Similar correlations were found in the earliest stages of the humic acid fouling experiments. A correlation of flux ratio with ΔG_{sw} can be observed in Figure 13 for the most selective membrane subset (FT-30, CD, and CE) for the humic acid fouling experiments.

Results for the most selective membrane subset in the humic acid fouling experiments were the only to show correlations over the entire monitoring period (i.e., for j_5, j_{20}, j_{35}, and j_{50}). Figure 14 indicates a correlation of J_{20} with ΔG_{sw} for the cellulose acetate membrane subset in the humic acid fouling experiments.

The slope of this trendline is much less than the trendline in Figure 13 because the three cellulose acetate membranes had more similar flux declines than did the three most selective membranes. In both Figures 13 and 14 a general correlation of increased fouling with increasing hydrophobicity (decreasing interfacial free energy) can be observed.

It can be concluded that in some cases, three-point correlations can be made between hydrophobicity and membrane performance for the two membrane subsets. However, no across-the-board correlations could be found between membrane hydrophobicity and flux decline. It is therefore concluded that membrane hydrophobicity may be better suited for inclusion in a larger model for membrane performance rather than used as an independent parameter. This conclusion will be further discussed in the conclusions section of this report.

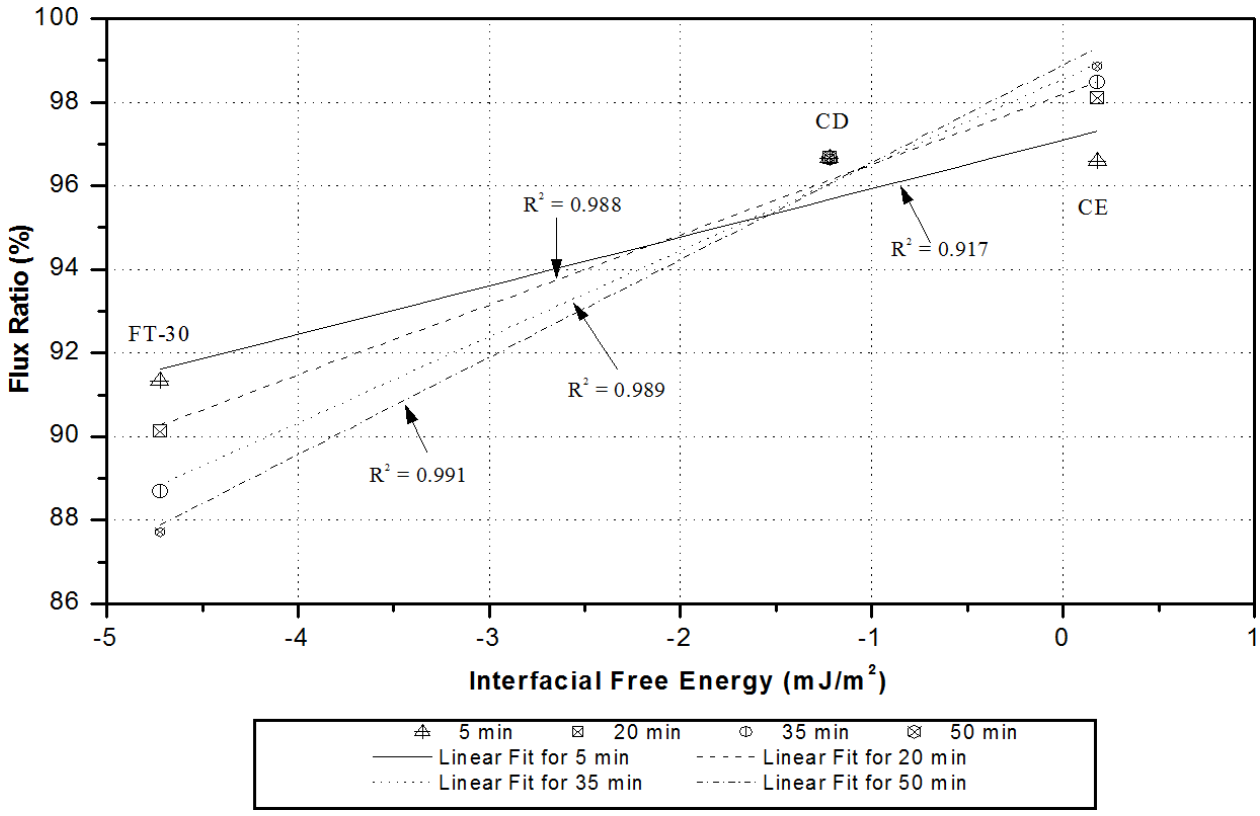

Figure 13.—Flux ratio as a function of interfacial free energy for the most selective membrane subset during PHA and $CaCl_2$ performance trials.

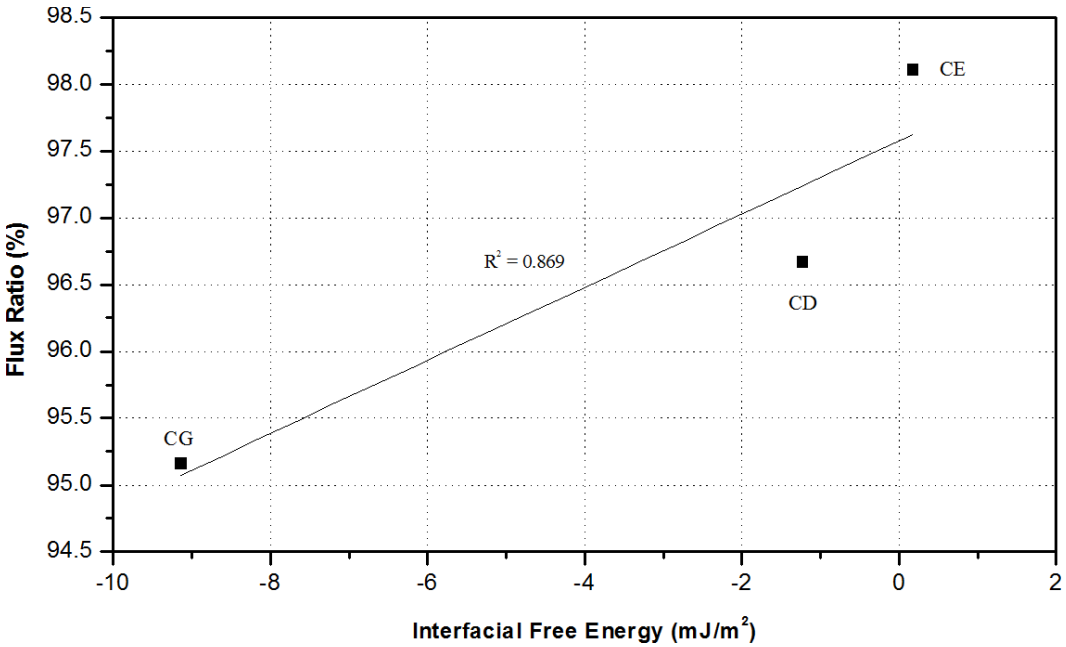

Figure 14.—Flux ratio at 20 minutes as a function of interfacial free energy for the cellulose acetate membrane subset during PHA and $CaCl_2$ performance trials.

5 CONCLUSIONS AND FUTURE RECOMMENDATIONS

5.1 Conclusions

The focus of this investigation was to develop a methodology for the determination of membrane hydrophobicity and to investigate possible relationships between membrane hydrophobicity and membrane fouling. Secondary objectives were to address the agreement between contact angles and membrane hydrophobicity and the best use of hydrophobicity data in predicting flux decline behavior.

5.1.1 Contact Angle Measurement

Protocol was established for the measurement of contact angles on both cellulose acetate and thin-film composite RO and NF membranes. Contact angles were measured using an automated goniometer and the captive bubble technique. Reproducible equilibrium contact angles were measured within 20 min after the air bubble is placed on the membrane surface.

Contact angles of the membranes were measured using three probe liquids (ultrapure water, glycerol, and diiodomethane). For the ultrapure water, glycerol, and diiodomethane, 95% confidence limits were ≤1.7°, ≤1.1°, and ≤2.2°,

respectively. According to values of contact angles with water, all of the membranes would be considered semi-hydrophilic because all of the contact angles fell within the 0° to 90° range.

5.1.2 Determination of Membrane Hydrophobicity

The contact angle measurements with the three probe liquids were then used in the Lifshitz-van der Waals/Acid-Base approach to quantitatively calculate the surface energetics of the membranes. The surface energy values were then used to quantitatively determine the hydrophobicity of the membranes. Three of the membranes were found to be hydrophobic and two were found to be hydrophilic. Comparing actual hydrophobicity calculations to hydrophobicity estimates from contact angle data, it was found that contact angle measurements are adequate for making relative hydrophobicity/hydrophilicity generalizations, but are not adequate for specific hydrophobicity/hydrophilicity determination.

5.1.3 Evaluating Relationships between Membrane Hydrophobicity and Membrane Performance

Determination of the role of hydrophobicity in membrane fouling was made difficult by the differences in surface roughness and porosity for the five membranes investigated. For this reason, correlations between membrane hydrophobicity and membrane fouling were evaluated in two subsets, each consisting of three membranes. Several three-point correlations were found for the earliest stages of the surfactant and humic acid fouling experiments. However, no across-the-board correlations that could be applied to all membranes and all solution chemistries could be found. For this reason, membrane hydrophobicity results may be better suited for inclusion in a larger model for membrane performance rather than used as an independent parameter.

5.2 Recommendations for Future Work

Based on observations made during this investigation, recommendations for future work have been developed. The recommendations pertain to improvements in the methodologies of the laboratory portion of the investigation as well as consideration for the best use of the resulting hydrophobicity data in predicting flux decline behavior.

5.2.1 Improvements to Methodology

Contact angle measurements were performed on the membrane surfaces prior to exposing them to a feed stream. However, because the foulant is added to the feed stream 45 hours after the membrane has been exposed to a 0.01 *M* NaCl, the foulant is encountering a surface that may be different from the one on which the contact angle measurements were originally performed. Therefore, contact angle

measurements should be performed on membranes that have been exposed to 0.01 *M* NaCl for 45 hours.

Contact angle measurements were made on the membrane surfaces with ultrapure water at pH ~ 5.6. However, one stipulation of the Lifshitz-van der Waals/Acid-Base approach, is that contact angles be measured on electrically neutral surfaces (van Oss 1993). Therefore, contact angle measurements for each membrane should be made with ultrapure water that has a pH adjusted to the pH of the isoelectric point of the respective membranes. The isoelectric point of the membrane can be determined from streaming potential measurements. It is anticipated that contact angle results with the pH-adjusted ultrapure water will not be substantially different from the contact angle results with ultrapure water at pH ~ 5.6.

The membranes were operated in a constant pressure, variable flux mode. Using flux ratios, the different permeation rates were normalized in order to compare flux decline for membranes with different initial flux values. However, it has been demonstrated that permeation rate significantly affects membrane fouling rate (Zhu and Elimelech 1995). Therefore, a better approach to comparing flux decline would be to operate all of the membranes in a constant flux, variable pressure mode. In this manner, all of the membranes would be exposed to a standardized foulant concentration at the interface. To create a membrane test unit capable of constant flux measurements, the membrane test unit in the current investigation would require several modifications. Constant flux is accomplished by providing a negative pressure head on the membrane using a peristaltic pump. In the modified membrane test unit, permeate lines from both test cells would be connected to a reservoir in which the negative pressure is controlled using a peristaltic pump at a set flowrate.

Further modifications, such as the addition of computer-interfaced flow meters on the permeate lines would allow for constant flow analysis. Constant flow analysis would enable continuous monitoring of the membrane fouling behavior; 15-min observation intervals would no longer be required. With continuous flow analysis, the performance measurement period could also be more easily extended in order to analyze longer term membrane fouling behavior.

5.2.2 Future Use of Hydrophobicity Data

In the extended DLVO model, the adhesion between a colloid and a membrane surface can be mechanistically examined. Traditionally, membrane-colloid interactions would be explained by the DLVO theory, which basically states:

total interaction = van der Waals + electric double layer

This does not take into account acid-base (hydrophobicity/hydrophilicity) interactions. However, the extended DLVO (van Oss 1993) takes the acid-base term into account and states:

total interaction = van der Waals + electric double layer + acid-base

or:

$$\Delta G_{1w2}^{TOT} = \Delta G_{1w2}^{LW} + \Delta G_{1w2}^{EL} + \Delta G_{1w2}^{AB}$$

where ΔG_{1w2}^{TOT} is the total free energy of attraction between a colloid (subscript 1) and the membrane (subscript 2) immersed in water (subscript w)

ΔG_{1w2}^{AB} is the acid-base component of the total free energy of attraction

ΔG_{1w2}^{LW} is the Lifshitz-van der Waals component of the total free energy of attraction

ΔG_{1w2}^{EL} is the electrostatic component of the free energy of attraction

The Lifshitz-van der Waals term (ΔG_{1w2}^{LW}) and the acid-base term (ΔG_{1w2}^{AB}) can be combined together into a single term, ΔG^{IF} (van Oss 1993):

$$\Delta G_{1w2}^{IF} = 2\left(\sqrt{\gamma_l^{LW}} - \sqrt{\gamma_1^{LW}}\right)\left(\sqrt{\gamma_2^{LW}} - \sqrt{\gamma_l^{LW}}\right) + 2\left[\begin{array}{l}\sqrt{\gamma_l^{+}}\left(\sqrt{\gamma_1^{-}} + \sqrt{\gamma_2^{-}} - \sqrt{\gamma_l^{-}}\right) + \\ \sqrt{\gamma_l^{-}}\left(\sqrt{\gamma_1^{+}} + \sqrt{\gamma_2^{+}} - \sqrt{\gamma_l^{+}}\right) - \\ \sqrt{\gamma_1^{+}\gamma_2^{-}} - \sqrt{\gamma_1^{-}\gamma_2^{+}}\end{array}\right]$$

where ΔG_{1w2}^{IF} is the interfacial component of the free energy of attraction

The surface tension values for water (subscript *w*) are known values, the surface tension values for the colloids (subscript 2) can be experimentally determined and the surface tension values for the membranes (subscript 2) can be determined by the method developed in the current investigation.

The electrostatic term, ΔG^{EL}, can be determined through electrokinetic measurements. Streaming potential measurements can be made on the membranes and electrophoretic mobility measurements can be made on the colloids. Summing the interfacial term and the electrostatic term results in the total free energy of interaction between the colloids and the membrane surface. For adsorption or adhesion of the colloids to occur, ΔG^{TOT} must be negative.

The overall objective of the future investigation would be to predict the fouling potential of typical colloidal feed streams on membrane surface characteristics by evaluating the fundamental surface characteristics of both the membrane and the colloids. This would have numerous implications for reducing membrane fouling,

including optimization of feed stream pretreatment (to change the colloid characteristics), modification of the membrane surface, or selection of the most appropriate membrane based on the feed stream characteristics.

6 REFERENCES

Adamson, A.W. 1960. *Physical chemistry of surfaces*, . New York: Interscience Publishers, Inc., 264 p.

Amirbahman, A., and T.M. Olson. 1995. Deposition kinetics of humic matter-coated hematite in porous media in the presence of Ca^{2+}. *Colloids and Surfaces A* 99 (1):1–10.

Bear, J. 1979. *Hydraulics of groundwater*. New York: McGraw Hill Inc., 191 p.

Belfort, G., R.H. Davis, and A.L. Zydney. 1994. The behavior of suspensions and macromolecular solutions in crossflow microfiltration. *J. Membrane Sci.* 96 (1):1–58.

Bhattacharyya, D., and M.E. Williams. 1992. Introduction and definitions—Reverse osmosis. In *Membrane handbook*, eds. W.S.W. Ho and K.K. Sirkar, 265–268. New York: Van Nostrand Reinhold.

Bouchard, C.R., J. Jolicoeur, P. Kouadio and M. Britten. 1997. Study of humic acid adsorption on nanofiltration membranes by contact angle measurements. *Canadian Journal of Chemical Engineering* 75:339–345.

Busscher, H.J, A.W.J Van Pelt, H.P De Jong, and J Arends. 1983. Effect of spreading pressure on surface free energy determinations by means of contact angle measurements. *Journal of Colloid and Interface Science* 95 (1):23–27.

Cadotte, J.E. 1985. Evolution of composite reverse osmosis membranes. In *Materials science of synthetic membranes*, ed. D.R. Lloyd, 273–294. Washington: American Chemical Society.

Capannelli, G., A. Bottino, V. Gekas, and G. Tragardh. 1990. Protein fouling behavior of ultrafiltration membranes prepared with varying degrees of hydrophilicity. *Process Biochemistry International* 25 (6):221–224.

Childress, A.E., and M. Elimelech. 1996. Effect of solution chemistry on the surface charge of polymeric reverse osmosis and nanofiltration membranes. *J. Membrane Sci.* 119 (2):253–268.

Childress, A.E. 1997. Characterization and performance of polymeric reverse osmosis and nanofiltration membranes. Ph.D. dissertation, University of California-Los Angeles.

Cuperus, F.P., and C.A. Smolders. 1991. Characterization of UF membranes—Membrane characteristics and characterization techniques. *Adv. Colloid Interface Sci.* 34:135–173.

Dahlgren, C., H. Elwing, and K.-E. Magnusson. 1986. Comparison of contact angles calculated from the diameter of sessile drops and submerged air bubbles in contact with a solid surface. *Colloids Surfaces* 17 (3):295–303.

Dann, J.R. 1970. Forces involved in the adhesive process: II. Nondispersion forces at solid-liquid interfaces. *Journal of Colloid and Interface Science* 32 (2):321–331.

Davis, R.H. 1992. Modeling of fouling of cross flow microfiltration membranes. *Separation and Purification Methods* 21:75–126.

Decker, E.L., B. Frank, Y. Suo, and S. Garoff. 1999. Physics of contact angle measurement. *Colloids and Surfaces A: Physiochemical and Engineering Aspects* 156 (1-3):177–189.

Denisov, G.A. 1994. Theory of concentration polarization in cross-flow ultrafiltration: Gel-layer model and osmotic-pressure model. *Journal of Membrane Science* 91 (1-2):173–187.

Drelich, J., and J. D. Miller. 1994. The effect of solid surface heterogeneity and roughness on the contact angle/drop (bubble) size relationship. *Journal of Colloid and Interface Science* 164 (1): 252–259.

Drelich, J., J.D. Miller, and R.J. Good. 1996. The effect of drop (bubble) size on advancing and receding contact angles for heterogeneous and rough solid surfaces as observed with sessile-drop and captive-bubble techniques. *Journal of Colloid and Interface Science* 179 (1):37–50.

Elimelech, M., W.H. Chen, and J.J. Waypa. 1994. Measuring the zeta (electrokinetic) potential of reverse osmosis membranes by a streaming potential analyzer. *Desalination* 95 (3):269–286.

Elimelech, M., X. Zhu, A.E. Childress, and S. Hong. 1997. Role of membrane surface morphology in colloidal fouling of cellulose acetate and composite aromatic polyamide reverse osmosis membranes. *J. Membrane Sci.* 127(1):101–109.

Extrand, C.W., and Y. Kumagai. 1996. Contact angles and hysteresis on soft surfaces. *Journal of Colloid and Interface Science* 184 (1):191–200.

Extrand, C.W. 1998. A thermodynamic model for contact angle hysteresis. *Journal of Colloid and Interface Science* 207 (1):11–19.

Fowkes, F.M. 1964. Attractive forces at interfaces. *Ind. Eng. Chem.* 56 (12):40–52.

Gekas, V., K.M. Persson, M. Wahlgren, and B. Sivik. 1992. Contact angles of ultrafiltration membranes and their possible correlation to membrane performance. *J. Membrane Sci.* 72:293–302.

Glater, J. 1998. The early history of reverse osmosis membrane development. *Desalination* 117 (1-3):297–309.

Good, R.J. 1979. Contact angles and the surface free energy of solids. In *Surface and Colloid Science, v. II: Experimental methods*, eds. R.J. Good and R.R. Stromberg, 1–29. New York: Plenium Press.

Good, R.J., and M.N. Koo. 1979. The effect of drop size on contact angle. *Journal of Colloid and Interface Science* 71 (2):283–292.

Gourley, L., M. Britten, S.F. Gauthier, and Y. Pouliot. 1994. Characterization of adsorptive fouling on ultrafiltration membranes by peptides mixtures using contact angle measurements. *J. Membrane Sci.* 97:283–289.

Grundke, K., T. Bogumil, C. Werner, A. Janke, K. Pöschel, H.-J. Jacobasch. 1996. Liquid-fluid contact angle measurements on hydrophilic cellulosic materials. *Colloids and Surfaces A: Physiochemical and Engineering Aspects* 116 (1-2):79–91.

Hamilton, W.C. 1972. A technique for the characterization of hydrophilic surfaces. *Journal of Colloid and Interface Science* 40 (2):219–222.

Hiemenz, P.C. 1986. *Principles of colloid and surface chemistry*. New York: Marcel Dekker, Inc., 287 p.

Hong, S., and M. Elimelech. 1997. Chemical and physical aspects of natural organic matter (NOM) fouling of nanofiltration membranes. *J. Membrane Sci.* 132 (2):159–181.

Jucker, C., and M.M. Clark. 1994. Adsorption of aquatic humic substances on hydrophobic ultrafiltration membranes, *J. Membrane Sci.* 97:37–52.

Keurentjes, J.T.F., J.G. Harbrecht, D. Brinkman, J.H. Hanemaaijer, M.A. Cohen Stuart, and K. van't Riet. 1989. Hydrophobicity measurements of microfiltration and ultrafiltration membranes. *J. Membrane Sci.* 47 (3):333–344.

Ko, Y.C., B.D. Ratner, A.S. Hoffman. 1981. Characterization of hydrophilic-hydrophobic polymeric surfaces by contact angle measurements, *Journal of Colloid and Interface Science* 82 (1):25–37.

Kulkarni, A., D. Mukherjee, and W.N. Gill. 1996. Flux enhancement by hydrophilization of thin film composite reverse osmosis membranes. *J. Membrane Sci.* 114 (1):39–50.

Kwok, D.Y., R. Lin, M. Mui, and A.W. Neumann. 1996. Low-rate dynamic and static contact angles and the determination of solid surface tensions. *Colloids and Surfaces A: Physiochemical and Engineering Aspects* 116 (1-2):63–77.

Kwok, D.Y., T. Gietzelt, K. Grundke, H.-J. Jacobasch, and A.W. Neumann. 1997. Contact angle measurements and contact angle interpretation. 1. Contact angle measurements by axisymmetric drop shape analysis and a goniometer sessile drop technique. *Langmuir* 13 (10):2880–2894.

Kwok, D.Y. and A.W. Neumann. 1999. Contact angle measurement and contact angle interpretation. *Advances in Colloid and Interface Science* 81 (3) 167–249.

Laîné, J.-M., J.P. Hagstrom, M.M Clark, and J. Mallevialle. 1989. Effects of ultrafiltration membrane composition. *J. Am. Water Works Assoc.* 81 (11):61–67.

Lee, L.H. 1999. Relevance of film pressures to interfacial tension, miscibility of liquids, and Lewis acid-base approach. *Journal of Colloid and Interface Science* 214, (1):64–78.

Majewska-Nowak, K., M. Kabsch-Korbutowicz, and T. Winnicki. 1997. Salt effect on the dye separation by hydrophilic membranes. *Desalination* 108 (1-3):221–229.

Mallevialle, J., P.E. Odendaal and M.R. Wiesner. 1996. The emergence of membranes in water and wastewater treatment. In *Water Treatment Membrane Processes*, eds. J. Mallevialle, P.E. Odendaal and M.R. Wiesner, 1.1–1.10. New York: McGraw-Hill.

Marmur, A. 1996. Equilibrium contact angles: Theory and measurement. *Colloids and Surfaces A: Physiochemical and Engineering Aspects* 116 (1-2):55–61.

Mukerjee, P and K.J. Musels. 1970. Critical Micelle Concentrations of Aqueous Surfactant Solutions. National Bureau of Standards.

Mukherjee, D., A. Kulkarni, and W.N. Gill. 1994. Flux enhancement of reverse osmosis membranes by chemical surface modification. *J. Membrane Sci.* 97:231–249.

Mukherjee, D., A. Kulkarni, and W.N. Gill. 1996. Chemical treatment for improved performance of reverse osmosis membranes. *Desalination* 104 (3):239–249.

Mulder, M. 1991. *Basic principles of membrane technology*. Dordrecht: Kluwer Academic Publishers.

Nabe, A., E. Staude, and G. Belfort 1997. Surface modification of polysulfone ultrafiltration membranes and fouling by BSA solutions. *Journal of Membrane Science* 133 (1) 57–72.

Neumann, A.W., and R.J. Good. 1979. Techniques of measuring contact angles. In *Surface and colloid science*, vol. 11, *Experimental methods*, ed. R. Good, 31–91. New York: Plenum Press.

Nyström, M., M. Laatikainen, K. Turku, and P. Järvinen. 1990. Resistance to fouling accomplished by modification of ultrafiltration membranes. *Progr. Colloid Polym. Sci.* 82:321–329.

Oldani, M., and G. Schock. 1989. Characterization of ultrafiltration membranes by infrared spectroscopy, ESCA, and contact angle measurements. *J. Membrane Sci.* 43 (2-3):243–258.

Petersen, R.J. 1993. Composite reverse osmosis and nanofiltration membranes. *J. Membrane Sci.* 83 (1):81–150.

Reihanian, H., C.R. Robertson, and A.S. Michaels. 1983. Mechanisms of polarization and fouling of ultrafiltration membranes by proteins. *Journal of Membrane Science* 16:237–258.

Rosa, M.J., and M.N. de Pinho. 1997. Membrane surface characterisation by contact angle measurements using the immersed method. *Journal of Membrane Science* 131 (1):167–180.

Sata, T., K. Mine, and M. Higa. 1998. Change in permselectivity between sulfate and chloride ions through anion exchange membrane with hydrophilicity of the membrane. *J. Membrane Science* 141 (1):137–144.

Song, L., and M. Elimelech. 1995a. Particle deposition onto a permeable surface in laminar flow. *J. Colloid Interface Sci.* 173 (1) 165–180.

Song, L., and M. Elimelech. 1995b. Theory of concentration polarization in crossflow filtration. *J. Chemical Society Faraday Trans.* 91:3389–3398.

van Oss, C.J., R.J. Good, and M.K. Chaudhury. 1986a. The role of van der Waals forces and hydrogen bonds in “hydrophobic interactions” between biopolymers and low energy surfaces. *Journal of Colloid and Interface Science* 111 (2):378–390.

van Oss, C.J., R.J. Good, and M.K. Chaudhury. 1986b. Solubility of proteins. *Journal of Protein Chemistry* 5 (6):385–405.

van Oss, C.J., and R.J. Good. 1988. Orientation of the water molecules of hydration of human serum albumin. *Journal of Protein Chemistry* 7(2):179–183.

van Oss, C.J. 1993. Acid-base interfacial interactions in aqueous media. *Colloids and Surfaces A* 78:1–49.

van Oss, C.J. 1994. *Interfacial forces in aqueous media*. New York: Marcel Dekker Inc., 440 p.

Williams, M.E., D. Bhattacharyya, R.J. Ray, and S.B. McCray. 1992. Reverse osmosis: Selected applications. In *Membrane Handbook*, eds. W.S.W. Ho and K.K. Sirkar, 312–354. New York: Van Nostrand Reinhold.

Wolanksky, G., and A. Marmur. 1998. The actual contact angle on a heterogeneous rough surface in three dimensions. *Langmuir* 14 (18):5292–5297.

Young, T. 1805. *Philos. Trans. R. Sci. London* 95:65.

Zhang, W., and B. Hallström. 1990. Membrane characterization using the contact angle technique, I. Methodology of the captive bubble technique. *Desalination* 79 (1):1–12.

Zhu, X.H., and M. Elimelech. 1995. Fouling of reverse osmosis membranes by aluminum oxide colloids. *J. Environ. Eng.* 121(12):884–892.

Zhu, X., and M. Elimelech. 1997. Colloidal fouling of reverse osmosis membranes: Measurements and fouling mechanisms. *Environmental Science & Technology* 31 (12):3654–3662.